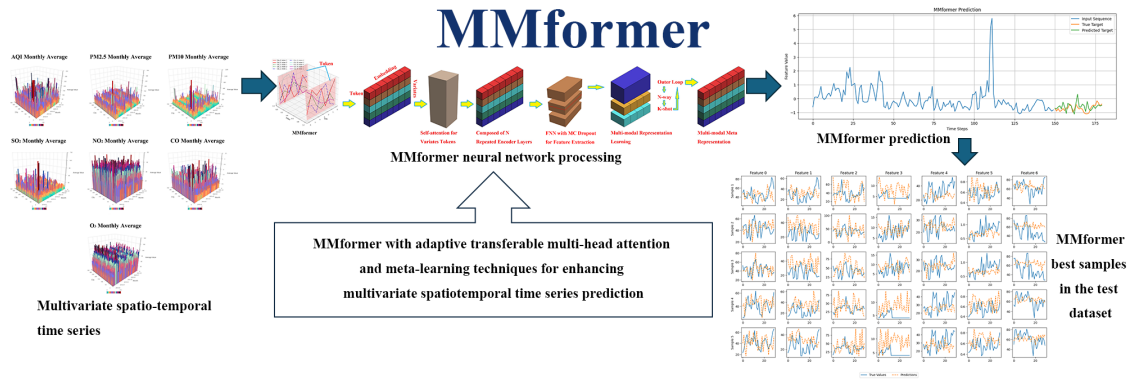


Graphical Abstract

MMformer with Adaptive Transferable Attention: Advancing Multivariate Time Series Forecasting for Environmental Applications

Ning Xin, Jionglong Su, Md Maruf Hasan



Highlights

MMformer with Adaptive Transferable Attention: Advancing Multivariate Time Series Forecasting for Environmental Applications

Ning Xin, Jionglong Su, Md Maruf Hasan

- Research Highlight 1

A novel MMformer model incorporating an adaptive transferable multi-head attention mechanism for multivariate time series prediction.

- Research Highlight 2

Combining self-attention with meta-learning improves the model's generalization ability and adaptability to different data distributions.

- Research Highlight 3

MMformer achieves state-of-the-art (SOTA) performance in multivariate time series, outperforming existing models such as iTransformer, Transformer, and SARIMAX.

MMformer with Adaptive Transferable Attention: Advancing Multivariate Time Series Forecasting for Environmental Applications

Ning Xin^a, Jionglong Su^a, Md Maruf Hasan^{a,*}

*^aSchool of AI and Advanced Computing, XJTLU Entrepreneur College (Taicang), Xi'an
Jiaotong-Liverpool University, Suzhou, 215123, Jiangsu, China*

Abstract

Environmental crisis remains a global challenge that affects public health and environmental quality. Despite extensive research, accurately forecasting environmental change trends to inform targeted policies and assess prediction efficiency remains elusive. Conventional methods for multivariate time series (MTS) analysis often fail to capture the complex dynamics of environmental change. To address this, we introduce an innovative meta-learning MTS model, MMformer with Adaptive Transferable Multi-head Attention (ATMA), which combines self-attention and meta-learning for enhanced MTS forecasting. Specifically, MMformer is used to model and predict the time series of seven air quality indicators across 331 cities in China from January 2018 to June 2021 and the time series of precipitation and temperature at 2415 monitoring sites during the summer (276 days) from 2012 to 2014, validating the network's ability to perform and forecast MTS data successfully. Experimental results demonstrate that in these datasets, the MMformer model reaching SOTA outperforms iTransformer, Transformer, and the widely used traditional time series prediction algorithm SARIMAX in the prediction of MTS, reducing by 50% in MSE, 20% in MAE as compared to others in air quality datasets, reducing by 20% in MAPE except SARIMAX. Compared with Transformer and SARIMAX in the climate datasets, MSE, MAE, and MAPE are decreased by 30%, and there is an improvement compared to iTransformer. This approach represents a significant advance in our ability to forecast and respond to dynamic environmental quality challenges in diverse urban and rural environments. Its predictive capabilities provide valuable public health and environmental quality information, informing targeted interventions.

1. Introduction

Deep learning (DL) has become a prevalent approach in multivariate time series (MTS) forecasting, driven by continual advancements in machine learning and its

*Corresponding author

Email addresses: Ning.Xin21@student.xjtlu.edu.cn (Ning Xin),
Jionglong.Su@xjtlu.edu.cn (Jionglong Su), MdMaruf.Hasan@xjtlu.edu.cn (Md Maruf Hasan
)

interdisciplinary applications. This progress has significantly enhanced MTS analysis using real-world data, leading to many impactful research contributions [1, 2]. Currently, MTS prediction is at the hot of research, focusing on deep learning-based forecasting, causal analysis, missing value imputation, and integrated heterogeneous MTS modeling [3, 4]. Despite these advancements, MTS analysis faces challenges, particularly related to high-dimensional data noise and complex correlations, which complicate model construction [5]. Additional issues include integrating datasets with varying sampling intervals and missing data [6], enhancing the interpretability of deep learning models [7], and addressing the unique characteristics and objectives of data from diverse domains [8].

MTS analysis primarily utilizes statistical modeling and deep learning methodologies [9], including Generative Adversarial Networks (GANs) [10] and Variational Autoencoders (VAEs) [11], to simulate and model data distributions. Recently, ensemble learning strategies that combine statistical techniques with machine learning algorithms have been proposed, creating hybrid models that use the strengths of both approaches [12]. Traditional statistical models, such as the Generalized Linear Model (GLM) [13], Seasonal Autoregressive Integrated Moving Average (SARIMA) [14], and Autoregressive Integrated Moving Average (ARIMA) [15], are valued for their interpretability and ability to identify linear temporal patterns with minimal data preprocessing. However, their effectiveness is reduced with complex datasets characterized by significant missing values and non-linear patterns. Conversely, machine learning methods like Gradient Boosting Machines (GBM) [16], Random Forests (RF) [17], and Support Vector Machines (SVM) [18] excel at identifying and predicting complex patterns to address challenges of traditional methods to complex data sets with nonlinear patterns but require extensive preprocessing, bringing challenges for users without advanced statistical expertise. Deep learning, a key subset of machine learning, addresses these limitations through its layered architecture and automatic feature learning capabilities. It enables effective non-linear representation and adaptability to diverse data structures to address limitations of traditional methods [19]. However, DL models are often computationally intensive and complex, limiting their practical application [20].

To overcome these challenges, this research introduces MMformer, a novel adaptive framework inspired by the iTransformer [21]. MMformer enhances MTS forecasting by efficiently utilizing temporal characteristics and time dependencies through innovative mathematical methods integrated within the neural network architecture, such as Bayesian inference combined with Meta-Learning. Structure features of MMformer include embedded variate tokens within the Feed Forward Network (FFN) [22] to identify hidden MTS characteristics and Monte Carlo Dropout (MC Dropout) [23] to reduce co-adaptation across network layers, thereby improving model robustness and regularization.

Additionally, MMformer uses an adaptive transferable multi-head attention mechanism, which combines multi-head attention with meta-learning [24]. This optimizes the encoder for various downstream tasks, enhancing the model’s efficiency and generalization capabilities. By effectively capturing temporal information and volatility structures, MMformer improves both predictive performance and processing efficiency.

To validate the effectiveness of MMformer, we apply it to model and predict the Air Quality Index (AQI) [25] and seven key pollutant indices [26] across 331 cities in China from January 2018 to June 2021 and precipitation and temperature patterns at 2415 monitoring sites during the summer (276 days) from 2012 to 2014 [27]. The results demonstrate MMformer’s state-of-the-art ability to handle environmental MTS data, offering enhanced forecasting accuracy and robustness compared to existing models.

The contributions of this work are as follows:

1. We propose MMformer, an innovative approach that integrates the dimension transpose with innovative Adaptive Transferable Multi-Head Attention (ATMA) and Bayesian approximate inference to better identify latent features in MTS data. This integration minimizes information loss and enhances representation learning, improving the ability to capture temporal patterns and forecasting accuracy.
2. We develop an advanced adaptive transferable multi-head attention module incorporating Model-Agnostic Meta-Learning (MAML). This design optimizes the attention mechanism, boosts model performance, reduces the need for manual tuning, and saves time.
3. Our MMformer is the first to demonstrate superior capability in long-term forecasting across various locations and multiple variables, particularly in predicting environmental issues, which is state-of-the-art performance. It also assists actuaries in optimizing insurance strategies for respiratory conditions and catastrophe insurance and supports government ecological policy-making.
4. Empirical analysis demonstrates that in air quality datasets, our approach significantly enhances predictive performance, reducing Mean Squared Error (MSE) by 50%, Mean Absolute Error (MAE) by 20%, and relative to other models except SARIMAX a 20% decrease in Mean Absolute Percentage Error (MAPE), our model outperforms Transformer and SARIMAX, achieving approximately 30% reduction in MSE, MAE, and MAPE metrics. Furthermore, better performance was observed in comparison with iTransformer. These findings substantiate the hypothesis that model efficacy correlates positively with feature dimensionality, suggesting that higher-dimensional feature spaces enable more robust predictive capabilities in MMformer.

The structure of this paper is organized as follows: Section 2 reviews MTS forecasting methods. Section 3 details the proposed approach. Section 4 presents the experimental design and results. Finally, Section 5 concludes and discusses future work.

2. Related Work

Advances in neural network architectures, particularly Transformer and its variants, have significantly elevated the prominence of multivariate time series (MTS) forecasting methodologies, catalyzing multidisciplinary research collaborations and

scholarly investigations across diverse domains [28, 29, 30, 31, 32]. This section presents a systematic review of the evolution of MTS forecasting techniques, tracing their development from conventional statistical approaches to contemporary neural network-based methods, thereby establishing the theoretical foundation for our proposed MMformer model.

2.1. Traditional Time Series Prediction

Early efforts in MTS forecasting mainly relied on statistical models such as Autoregressive Integrated Moving Average (ARIMA) [33] and Seasonal ARIMA (SARIMA) [34]. These models are experts in capturing linear dependencies in univariate time series data but face significant limitations when extended to multivariate settings [35, 36, 37]. Specifically, ARIMA and SARIMA struggle with the increased complexity and computational demands of modeling multiple interrelated variables [38]. Furthermore, these models operate under the restrictive stationary assumption, requiring the statistical properties of the time series to remain constant over time, which is often violated in real-world multivariate data [?]. Similarly, Exponential Smoothing [33] is simple and offers interpretability but is constrained by high-dimensional data, relies on stationary or locally stationary processes, and fails to capture nonlinear relationships effectively [39].

2.2. Multivariate Time Series Prediction

To address the limitations of univariate models, multivariate approaches like Vector Autoregression (VAR) [40] and State Space Models (SSMs) [41] have been introduced. VAR models extend the autoregressive framework to multiple variables, allowing for the capture of interdependencies among different MTS [42]. Despite their theoretical appeal, VAR encounters challenges related to high dimensionality, significantly as the number of variables increases, leading to computational inefficiency and overfitting [43]. While flexible in representing dynamic systems, SSMs often require extensive computational resources and expertise to specify appropriate latent structures, making them less accessible for large-scale applications [44].

2.3. Machine Learning in Time Series Prediction

The advent of machine learning techniques brought new perspectives to MTS forecasting [12]. Support Vector Machines (SVMs) [45] and the Multilayer Perceptron (MLP) [46] as popular choices due to their ability to model complex, nonlinear relationships without extensive parameter tuning. These methods improved prediction accuracy compared to traditional statistical models [47]. However, they lack mechanisms to capture temporal dependencies effectively, necessary for MTS data [47, 48]. Additionally, feature engineering becomes a prerequisite to harness temporal information, adding to the complexity of model development [12].

2.4. Deep Learning in Time Series Prediction

Recent advancements in MTS analysis, with more researchers moving away from traditional MTS forecasting to explore machine learning and neural network methodologies [35, 49, 50].

Deep learning models, particularly Recurrent Neural Networks (RNNs) [51] and Long Short-Term Memory networks (LSTMs) [52], changed MTS forecasting by

modeling temporal dependencies. RNNs introduced the capability to retain information over sequences [53], while LSTMs reduced the vanishing gradient problem, enabling the capture of long-range dependencies [54]. Despite these advancements, RNN-based models require many computational resources and training time [6]. Furthermore, they often struggle with parallelization, limiting their scalability for large datasets and real-time forecasting applications [55, 56].

2.5. Transformer in Time Series Prediction

The introduction of Transformer architectures represented a substantial advancement in MTS forecasting [57]. Models such as the Temporal Fusion Transformer (TFT) [58] and Informer [59] leveraged self-attention mechanisms to capture dependencies across different time steps efficiently [28]. These models offer advantages in handling long-range dependencies and parallel processing, resulting in faster training times and improved scalability [57]. However, challenges remain in optimizing self-attention for MTS and effectively integrating diverse data modalities to enhance prediction accuracy [60, 61].

2.6. Structured Diversity in Time Series Prediction

While simple and interpretable, traditional MTS models often struggle with non-linear and complex data [62]. In contrast, neural networks offer improved predictions for such data but require extensive training and careful parameter selection to avoid overfitting [35]. Integrating structural diversity allows models to capture a broader range of patterns and interactions within the data, reduce individual model biases, and improve robustness [63]. However, for complex, real-world datasets, neural networks are often the preferred forecasting tool [64, 65]. Despite these benefits, effectively combining diverse structures remains complex, requiring complicated architectures and extensive computational resources.

2.7. MMformer: Advancing Multivariate Time Series Prediction

Based on the concept in the iTransformer [21] and addressing the Transformer’s limitations in time series prediction, the proposed MMformer introduces a novel approach to MTS forecasting. Meta-learning helps enhance time series forecasting when data is limited [66]. The Meta-Learning-based prediction mechanism for few-shot time series forecasting demonstrates superior accuracy and convergence speed, surpassing models trained directly on targeted task-specific MTS datasets [67]. Therefore, MMformer integrates the adaptive transferable multi-head attention with the iTransformer’s dimension transpose for high-dimensional, nonlinear data, incorporating spatial dependencies alongside temporal dynamics. By effectively capturing multiple data patterns and using structural diversity, MMformer enhances prediction accuracy and scalability. Furthermore, it optimizes computational efficiency, making it suitable for real-time applications. Through these innovations, MMformer addresses the challenges posed by traditional and contemporary models, offering a robust solution for complex air quality forecasting tasks.

3. Methodology

This section is organized as follows: Section 3.1 describes the data preprocessing methods and formats. Section 3.2 comprehensively describes the methodology, including detailed procedures and clear flowcharts. Section 3.3 focuses on the model's components, detailing the innovative components. This algorithm integrates MC Dropout regularization techniques and introduces an innovative adaptive multi-head attention mechanism. These advancements lead to substantial improvements in neural network optimization and increase the accuracy of time-series forecasting.

3.1. Data Preprocessing

This study used a comprehensive data preprocessing step to ensure the quality and consistency of the MTS data input to the model. Fig.1 is the flowchart of data preprocessing, and the preprocessing process includes the following key steps:

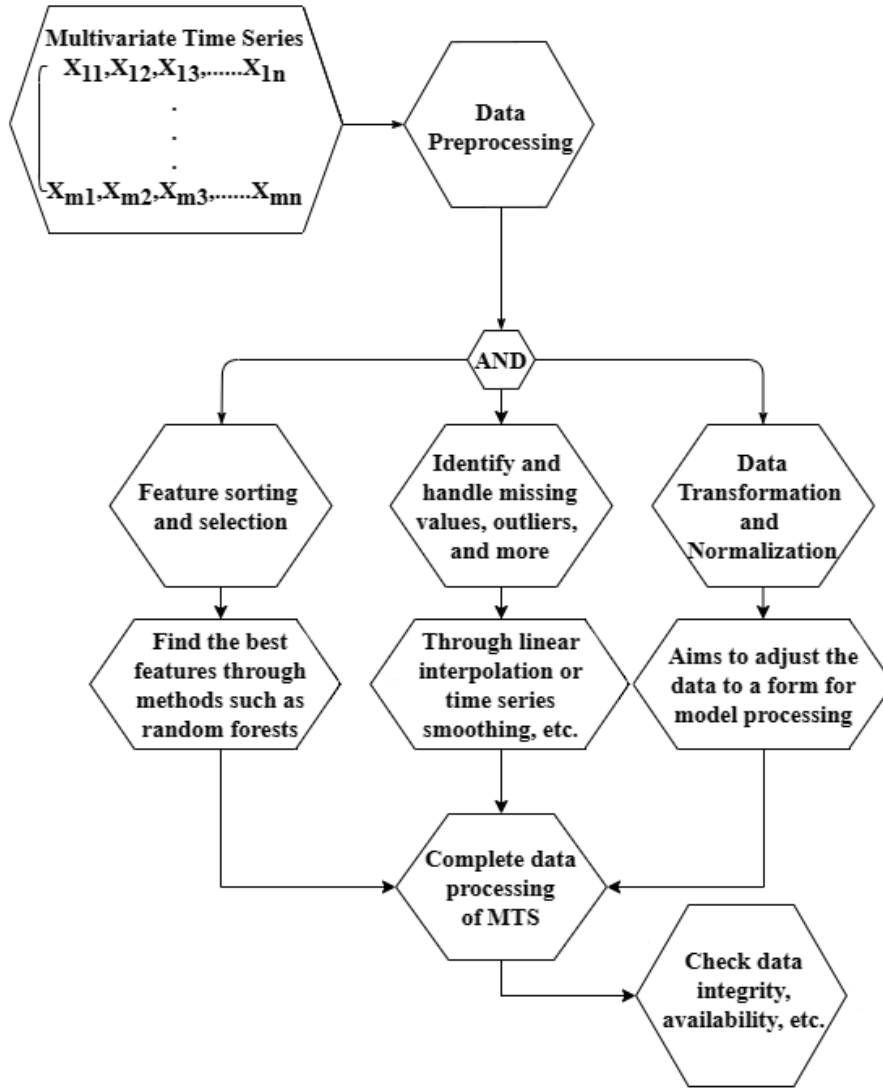


Figure 1: Flowchart of Data Preprocessing

- Step 1. Feature sorting and selection: Features are sorted and selected using random forests to identify the prediction task’s most relevant and influential features. This step helps to reduce noise and improve the efficiency and accuracy of the model.
- Step 2. Missing value and outlier processing: Missing values and outliers in the dataset are treated using techniques such as linear interpolation or MTS smoothing to ensure the continuity and reliability of the data.
- Step 3. Data transformation and normalization: The selected features are subjected to necessary data transformation and normalization. This step aims to adjust the data to a form suitable for model processing.
- Step 4. Integrity check: In the final stage of preprocessing, the processed data is checked for integrity, including verification of data integrity, availability, etc., to ensure that the data quality meets the requirements of model training.

3.2. Workflow Overview

This subsection outlines our research methodology, illustrated by the flow diagrams in Fig.2.

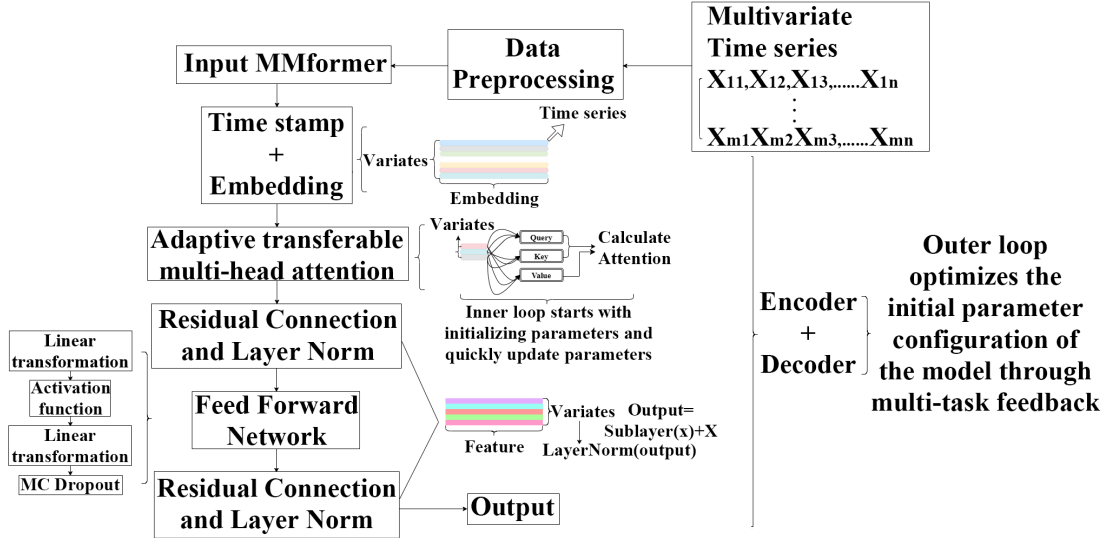


Figure 2: MMformer neural network flow chart, describing the core operating principle of the model and the operation mode of adaptive transferable multi-head attention

The MMformer uses datasets for automatic feature extraction and employs meta-learning during training to identify key sequence segments for predicting temporal patterns.

Initially, the MTS data undergoes preprocessing. Subsequently, The MMformer uses a sliding-window function to segment each city’s time series into input sequences and subsequent prediction targets, effectively creating additional subsets from the original MTS data, allowing the model to capture diverse patterns and enhance robustness and generalization.

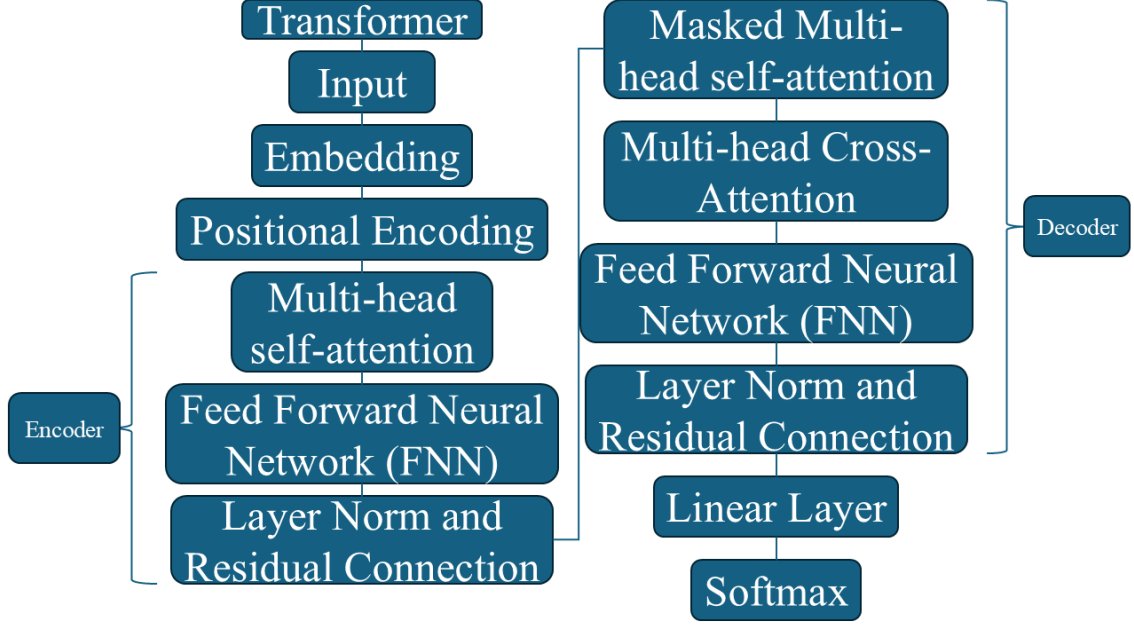


Figure 4: Transformer structure

variance, respectively. The purpose of expressing this operation in set form is to emphasize that standardization occurs separately for each time step (token). This set representation indicates that the same normalization procedure is applied independently to each time step n . The MMformer uses Multi-Layer Perceptrons (MLPs) for embedding and mapping layers, eliminating the need for positional encoding by independently mapping sequences to variate tokens and introducing time encoding.

MMformer enhances MTS analysis by integrating embedding methodology while retaining time positional encoding, thereby improving the processing of diverse inputs. Central to MMformer is the Adaptive Transferable Multi-Head Attention (ATMA) proposed by us, which advances traditional multi-head self-attention by dynamically adjusting attention parameters and enabling transfer learning across various tasks. The architecture incorporates multiple linear and affine mapping layers (Eq.2) within its feedforward network (FFN) and employs Monte Carlo Dropout (Eqs.3 and 4) instead of standard Dropout to capture richer feature representations:

$$y = Wx + b, \quad (2)$$

where W and b are the weight matrix and bias vector, x is the input, and y is the output. During inference, multiple stochastic forward passes with dropout produce the average prediction \hat{y} :

$$\hat{y} = f(x; \theta, \text{dropout}), \quad (3)$$

By performing multiple stochastic forward passes (e.g., T times) to obtain the average prediction \bar{y} :

$$\bar{y} = \frac{1}{T} \sum_{t=1}^T \hat{y}^t, \quad (4)$$

where \hat{y}^t represents the output from the t -th pass with dropout applied.

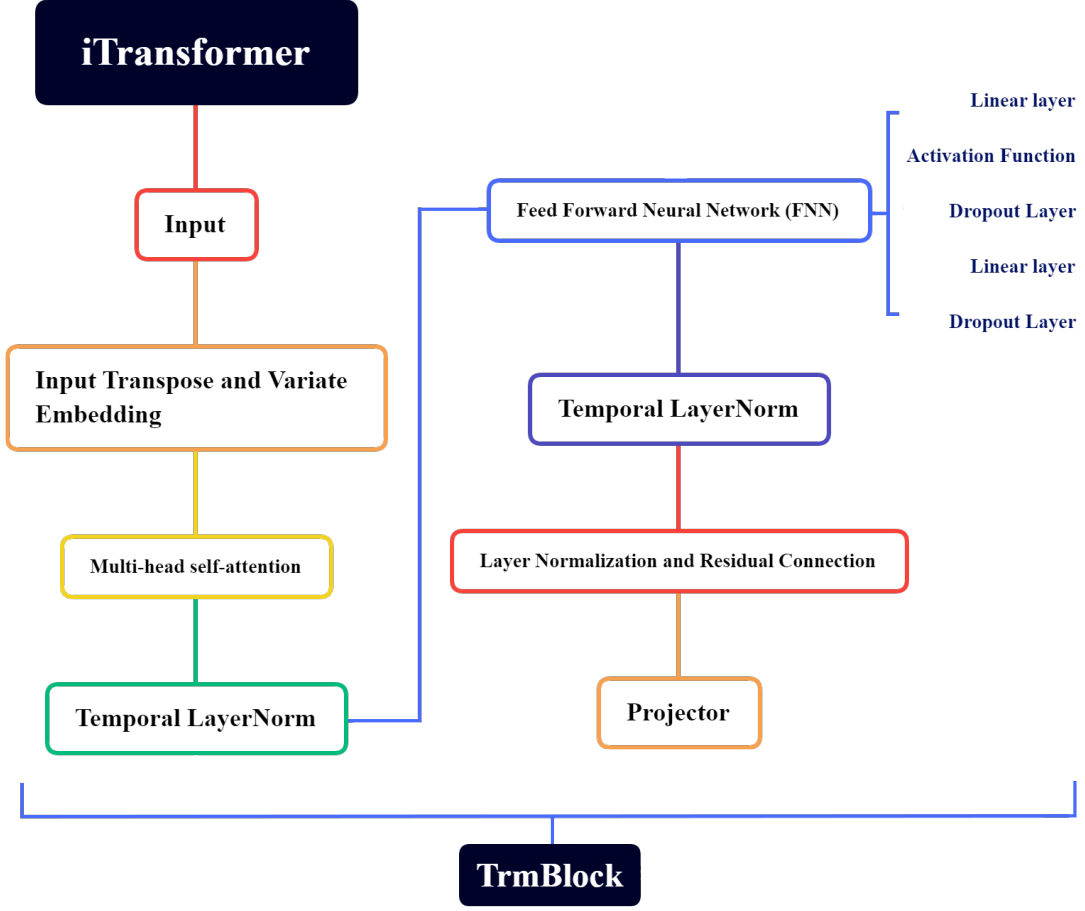


Figure 5: iTransformer structure

Designed for versatility, MMformer addresses various multivariate time series tasks, demonstrating robust adaptability and transfer learning capabilities.

3.3.2. Adaptive transferable multi-head attention

The self-attention mechanism, fundamental to the Transformer architecture, encodes each input sequence element as a high-dimensional vector [68]. For a sequence $X = (x_1, x_2, \dots, x_n)$, linear transformations generate query Q , key K , and value V vectors as $Q = XW_Q$, $K = XW_K$, and $V = XW_V$.

The attention weight $\alpha^{(i,j)}$ between query q_i at position i and key k_j at position j is computed using the scaled dot-product:

$$\alpha^{(i,j)} = \frac{q_i \cdot k_j}{\sqrt{d_k}}, \quad (5)$$

where d_k is the dimension of q_i . This scaling mitigates the softmax gradient issues for small values. The weights are then normalized via softmax:

$$\alpha^{(i,j)} = \text{softmax}(\alpha^{(i,j)}). \quad (6)$$

The normalized weights $\alpha^{(i,j)}$ determine the contribution of each value vector v_j to

the representation h_i at position i :

$$h_i = \sum_j \alpha^{(i,j)} v_j. \quad (7)$$

Where Eq.7 multiplies the normalized attention weight $\alpha^{(i,j)}$ and the vector v_j and sums each product up to obtain the weighted sum representation h_i of the position i . It can be seen as a weighted sum of the vectors of all positions, and the weight is $\alpha^{(i,j)}$.

Different from the standard Transformer, iTransformer's self-attention focuses on inter-variable rather than temporal correlations:

$$\text{Attention}(Q, K, V) = \text{softmax}\left(\frac{QK^\top}{\sqrt{d_v}}\right) V, \quad (8)$$

where d_v is the dimensionality of the value vectors, while the mathematical formulations are similar, iTransformer emphasizes variable relationships over time steps, enhancing its capability to model complex multivariate dependencies.

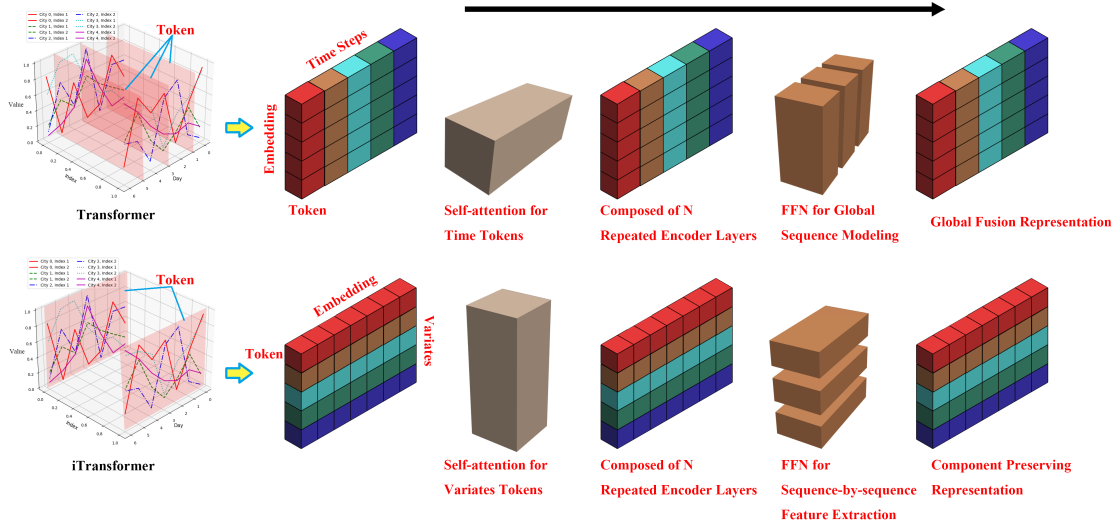


Figure 6: Comparison between Transformer and iTransformer architectures

Fig.6 illustrates the distinct implementations of Transformer and iTransformer. Traditional Transformers aggregate multiple variables from a single time step into one token, capturing temporal dependencies but potentially hiding variable interactions. In contrast, iTransformer embeds each variable's entire MTS into separate tokens, allowing the attention mechanism to effectively capture inter-variable correlations. This approach facilitates non-linear representations through feed-forward networks, enhancing variable-centric learning and mitigating limitations associated with mixed time tags and limited receptive fields.

Fig.7 and 8 highlight that in contrast to Transformer and iTransformer, the MMformer structure assigns independent tokens to each variable and incorporates the Adaptive Transferable Multi-Head Attention (ATMA) mechanism. ATMA integrates meta-learning to enhance multimodal data integration, capturing complex

inter-variable relationships through multi-head attention. This design improves MMformer’s ability to process MTS, maintaining robustness on small datasets or those with outliers, and only requires minimal parameter tuning.

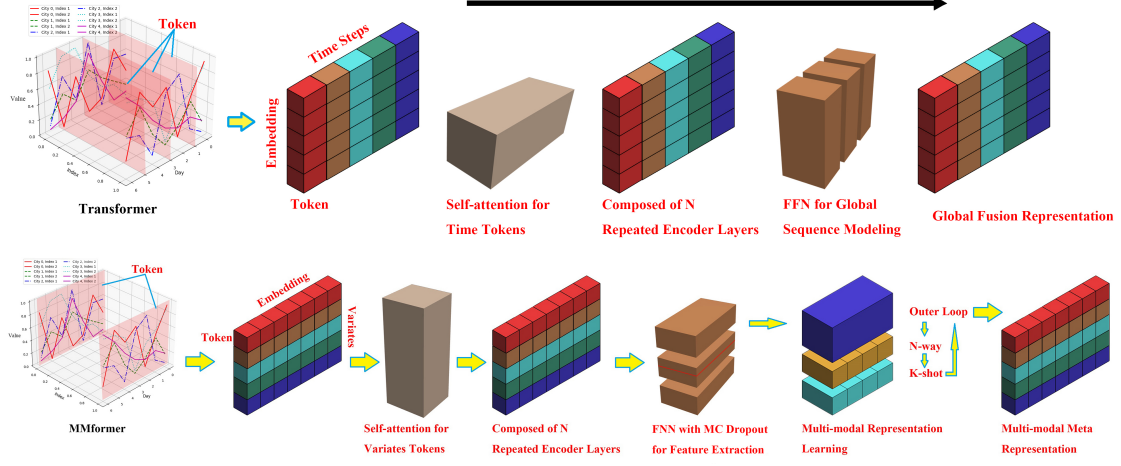


Figure 7: Comparison between Transformer and MMformer. ATMA performs forward propagation on input tasks, calculates the current batch’s loss, and accumulates it in task loss to adapt parameters to the current task. The adapted parameters are forward propagated to obtain outputs, and meta loss is calculated between outputs and targets. Meta loss is used in the outer loop to update the model’s meta parameters, while the current epoch’s validation set loss is used to update the model.

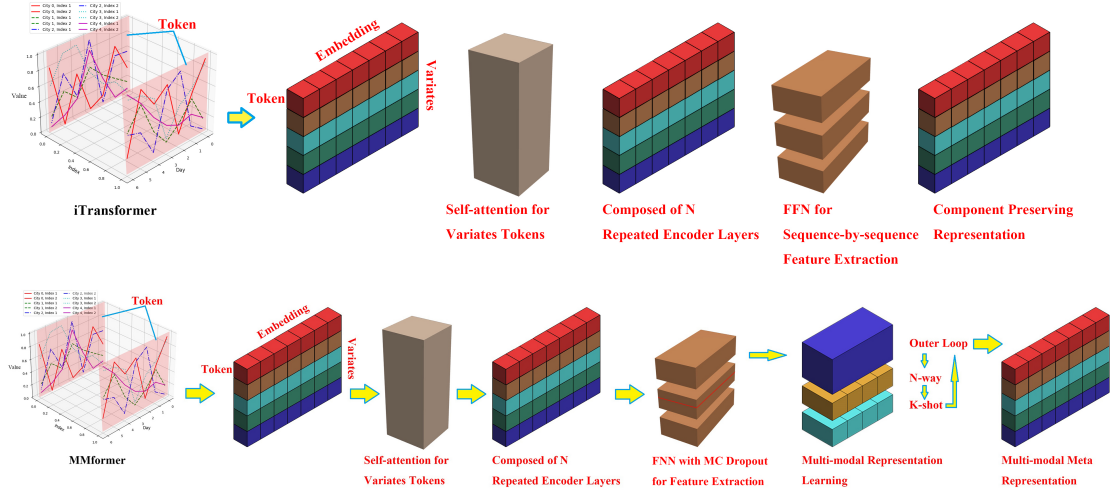


Figure 8: Comparison between iTransformer and MMformer

The ATMA framework defines a set of tasks \mathcal{T} , where each task $T_i \in \mathcal{T}$ includes a loss function \mathcal{L}_{T_i} , initial observation distribution $q(x_1)$, transition distribution $q(x_{t+1}|x_t, a_t)$, and designated time step H_i . A task T_i is randomly selected, and model parameters θ are updated to θ'_i via gradient descent using loss function \mathcal{L}_{T_i} :

$$\theta'_i = \theta - \alpha \nabla_{\theta} \mathcal{L}_{T_i}(f_{\theta}(x_{T_i}), y_{T_i}). \quad (9)$$

where θ denotes the initial parameters for the current meta-iteration. θ'_i denotes the updated model parameters for task T_i using task-specific data in the inner loop, and the adjustments at the task level are implicit, primarily focusing on updating the meta-parameters θ rather than directly computing or using each θ'_i . α is the task-level learning rate that controls the model’s learning step size on a single task. \mathcal{L}_{T_i} is the loss function of task T_i used to evaluate the f_θ performance on that task. $\nabla_\theta \mathcal{L}_{T_i}(f_\theta(x_{T_i}), y_{T_i})$ is the gradient of the loss function \mathcal{L}_{T_i} to the model parameters θ , where x_{T_i} and y_{T_i} represent the input data and target output of task T_i respectively.

The aim of this step is to optimize the parameter θ such that the sum of the loss functions across all tasks in the task set \mathcal{T} is minimized, i.e., $\min_\theta \sum_{T_i \sim \mathcal{T}} \mathcal{L}_{T_i}(f_\theta(x_{T_i}), y_{T_i})$, where the notation \sim indicates that tasks T_i are sampled from the task set \mathcal{T} . The objective is to minimize the cumulative loss across all tasks:

$$\theta \leftarrow \theta - \beta \nabla_\theta \sum_{T_i \sim \mathcal{T}} \mathcal{L}_{T_i}(f_\theta(x_{T_i}), y_{T_i}), \quad (10)$$

where β is the meta-learning rate, which controls the learning step length of the model on multiple tasks. Eq.14 leverages the gradients obtained from all sampled tasks T_i during the inner loop (Eq.13) to adjust the meta-parameters θ . In the outer loop, the overall model parameters θ are updated by aggregating the meta-gradients from multiple tasks, each adjusted by a specific learning rate β . Consequently, there is no single formula for θ' , as it represents an intermediate result for each task during the inner loop execution.

The meta-learning objective function is:

$$\sum_{T_i \sim \mathcal{T}} \mathcal{L}_{T_i}(f_{\theta - \alpha \nabla_\theta \mathcal{L}_{T_i}(f_\theta(x_{T_i}), y_{T_i})}), \quad (11)$$

where aiming to find optimal θ that minimizes the cumulative loss through iterative inner loop (Eq. 13) and outer loop (Eq. 14) updates that reduce the cumulative loss across all tasks in the task set \mathcal{T} .

The proposed ATMA mechanism combines self-attention with meta-learning to enhance MTS analysis. By defining a diverse task set and performing gradient updates per task, ATMA enables rapid model adaptation and improves generalization across tasks through meta-gradients. This integration extends self-attention to multi-dimensional long and short-term sequences, resulting in the MMformer model. MMformer has robustness on limited or noisy datasets while remaining user-friendly for researchers lacking tuning experience. ATMA’s innovative design offers significant potential for advancements in related domains.

4. Experiments Application and Results

This section employs the MMformer to analyze two datasets. The datasets, sourced from the China Meteorological Data Service Center under the National Meteorological Information Center [27], encompass comprehensive raw data essential for accurate forecasting and detecting trends. We benchmark MMformer against iTransformer, Transformer, and SARIMA models to demonstrate its superior performance.

This evaluation provides insights into MMformer’s effectiveness as the MTS prediction tool for environmental monitoring.

4.1. Multivariate Time Series Data Display

The proposed MMformer model’s effectiveness in predicting air quality using daily average measurements of seven indicators across 331 Chinese cities over 1,277 days (January 2018 to June 2021) and temperature patterns at 2415 monitoring sites during the summer (276 days) from 2012 to 2014. This research uses daily average values for seven air quality indicators rather than instantaneous measurements, which reduces the impact of transient phenomena on prediction outcomes. While air quality data contains ephemeral fluctuations, such as short-term pollution peaks or rapid meteorological changes induced, these phenomena are effectively smoothed in daily average aggregations, reducing extreme values’ influence on overall trends.

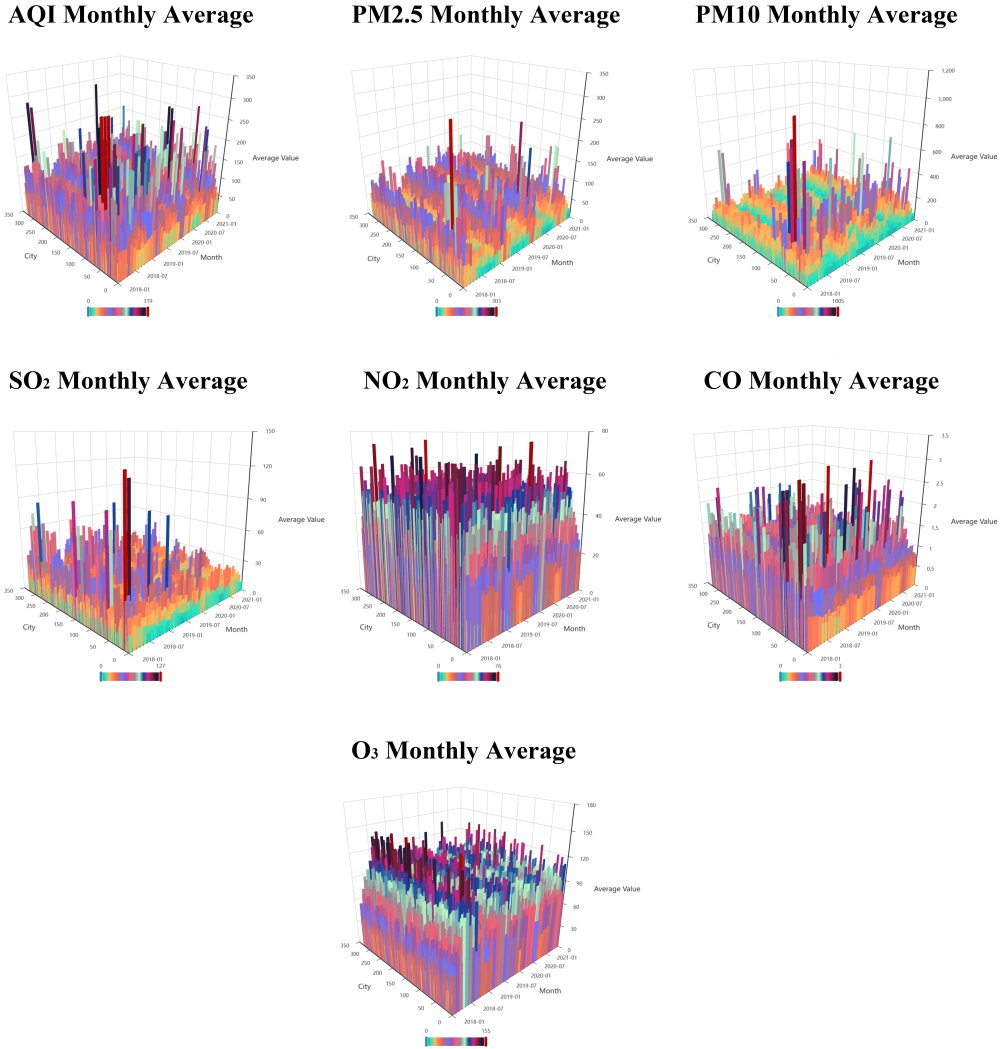


Figure 9: Air Quality Data from January 2018 to Jun 2021

Fig.9 depicts the monthly air quality average values of each indicator in all cities to illustrate the general distribution and outliers of the data, providing a general

understanding. The horizontal and vertical axes represent the city number, the corresponding month, and the monthly average value of the city at that time.

Table 1: Summary of features from meteorological MTS data of weather stations

Feature	Description
AQI	Air quality index
PM2.5	Fine particulate matter less than or equal to 2.5 microns in diameter
PM10	Inhalable particulate matter with a diameter less than or equal to 10 microns
SO ₂	Sulfur dioxide can cause respiratory
NO ₂	Nitrogen dioxide can cause respiratory tract irritation
CO	Carbon monoxide impair oxygen transport
O ₃	Ozone will irritate the respiratory

Table 1 summarizes the seven air quality indicators. After initial processing, the dataset’s features are detailed in Table 2, laying the foundation for subsequent analysis, which combines with Fig.9 we can observe the value ranges of the seven features vary greatly, and the mean, median, and 25% quartile do not fluctuate much within four years, while the maximum values of some indicators change significantly.

Table 2: Summary of Air Quality Statistics about 7 indexes

Indicator	Maximum Value	25% QUARTILE	Mean	Median
2018 AQI	500	45	71	61
2019 AQI	500	43	67	58
2020 AQI	500	33	57	48
2021 AQI	500	37	65	54
2018 PM2.5	1787	19	39	30
2019 PM2.5	1348	19	38	30
2020 PM2.5	1188	15	33	25
2021 PM2.5	1399	17	36	28
2018 PM10	5850	38	76	58
2019 PM10	4709	38	70	58
2020 PM10	2767	30	60	48
2021 PM10	6593	34	77	55
2018 SO ₂	251	6	13	10
2019 SO ₂	241	6	11	9
2020 SO ₂	142	5	10	8
2021 SO ₂	432	5	10	8
2018 NO ₂	163	16	27	24

Continued on next page

Table 2 – *Summary of Air Quality Statistics about 7 indexes*

Indicator	Maximum Value	25% QUAR-TILE	Mean	Median
2019 NO ₂	131	16	28	25
2020 NO ₂	125	14	25	21
2021 NO ₂	152	14	24	22
2018 CO	6.88	0.59	0.85	0.76
2019 CO	5.49	0.57	0.80	0.73
2020 CO	26.42	0.51	0.73	0.66
2021 CO	13.76	0.50	0.71	0.65
2018 O ₃	245	42	65	62
2019 O ₃	276	40	61	58
2020 O ₃	218	41	62	60
2021 O ₃	216	45	64	62
2018-2021 AQI	500	40	65	56
2018-2021 PM2.5	1787	17	37	28
2018-2021 PM10	6593	35	70	54
2018-2021 SO ₂	432	6	11	8
2018-2021 NO ₂	163	15	26	23
2018-2021 CO	26.42	0.55	0.78	0.71
2018-2021 O ₃	276	42	63	60

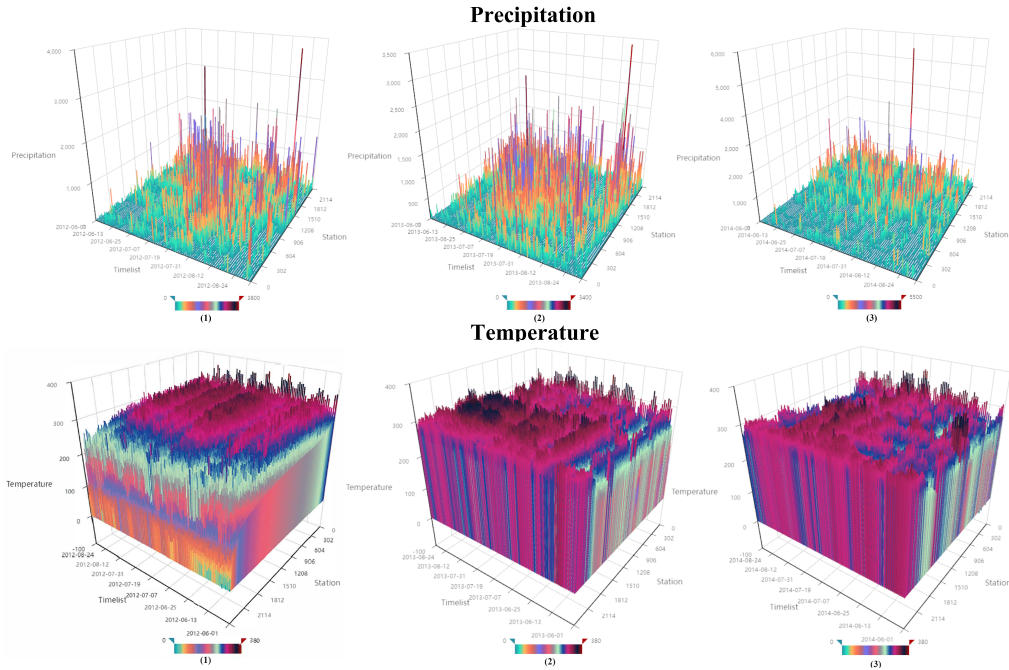


Figure 10: Precipitation and Temperature from 2012 to 2014 June-August

Fig.10 presents a comprehensive visualization of data distribution patterns and outlier occurrences. The color gradient bar beneath each graph corresponds to tem-

perature and precipitation values. The horizontal axis denotes temporal progression and station identification numbers, while the vertical axis represents temperature or precipitation measurements. Analysis reveals highly heterogeneous summer rainfall distribution across the three years, contrasted with consistently rising temperatures. Table 3 provides a statistical summary of the processed dataset, encompassing precipitation and temperature metrics within the climate dataset.

Table 3: Summary of Weather Station Statistics about Precipitation and Temperature

Indicator	Maximum	Minimum	Mean	NSBM ¹
Total Precipitation²	115	0	23	1357
2012 Precip	137	0	24	1391
2013 Precip	119	0	24	1407
2014 Precip	121	0	22	1415
Total Temperature³	301	121	243	1011
2012 Temp	328	55	242	987
2013 Temp	320	48	249	986
2014 Temp	315	46	239	949

¹ Number of sites below mean

² The unit of precipitation: 0.1mm

³ The unit of temperature: 0.1°C

4.2. Evaluation Baseline Metrics

Appropriate evaluation metrics are essential to assess the performance of various models in MTS prediction tasks. This study employs Mean Absolute Error (MAE), Mean Squared Error (MSE), and Mean Absolute Percentage Error (MAPE) as the primary indicators, each providing distinct insights into prediction accuracy and deviation.

- **Mean Absolute Error (MAE)** [69]: MAE calculates the average absolute differences between predicted and actual values, offering a straightforward measure of prediction accuracy. A lower MAE indicates better model performance.

$$\text{MAE} = \frac{1}{n} \sum_{i=1}^n |y_i - \hat{y}_i| \quad (12)$$

where y_i are the actual values, \hat{y}_i the predicted values, and n the number of observations.

- **Mean Squared Error (MSE)** [69]: MSE measures the average of the squared differences between predicted and actual values, making it sensitive to larger errors. This sensitivity helps identify models with lower variance in their predictions.

$$\text{MSE} = \frac{1}{n} \sum_{i=1}^n (y_i - \hat{y}_i)^2 \quad (13)$$

Each error $(y_i - \hat{y}_i)$ is squared in this formula, amplifying more significant errors. This means the MSE heavily penalizes significant deviations from the actual values, highlighting models with lower prediction variance.

- **Mean Absolute Percentage Error (MAPE)** [70]: MAPE expresses the accuracy as a percentage, facilitating easy comparison across different datasets. It calculates the average absolute percentage deviations between predicted and actual values, with lower values indicating higher accuracy.

$$\text{MAPE} = \frac{1}{n} \sum_{i=1}^n \left| \frac{y_i - \hat{y}_i}{y_i} \right| \times 100\% \quad (14)$$

4.3. Application Analysis on Datasets

The predictive analysis of data consists mainly of two stages: fundamental statistical analysis and comparison of the prediction performance of various methods.

4.3.1. Basic Statistical Analysis of Data

Table 4 and Table 5 summarise the statistics of key indicators in the air quality and climate datasets.

Table 4: Basic statistical analysis of air quality characteristic indicators

Indicator	Mean	Variance	Max	Min	Median
AQI	65	1842	500	0	56
PM2.5	37	1076	1787	0	28
PM10	70	5797	6593	0	54
SO₂	11	88	432	0	8
NO₂	26	231	163	0	23
CO	0.78	0.14	26.42	0	0.71
O₃	63	847	276	0	60

Table 5: Basic statistical analysis of temperature and precipitation characteristic indicators

Indicator	Mean	Variance	Mode	Range	IQR ¹
Precipitation²					
2012³	25.29	8744.63	0	3733	4.00
2013	25.00	8276.23	0	3391	2.00
2014	22.99	7643.99	0	5431	3.00
Temperature⁴					
2012	242.36	2147.62	262	380	59.00
2013	248.57	2432.61	280	383	64.00
2014	239.31	2084.03	249	423	57.00

¹ Interquartile range

² The unit of precipitation: 0.1mm

³ The unit of time: year

⁴ The unit of Temperature: 0.1°C

Based on Table 4 analysis, all air quality features show minimum values of 0, with significant variance across all indicators except *CO*, indicating substantial regional air quality disparities. The consistently lower median values compared to means suggest right-skewed distributions, where generally good air quality is punctuated by severe pollution events. These spatial and temporal variations in pollution levels underscore the necessity for robust, targeted monitoring systems in high-risk areas.

From Table 5, 2013 precipitation data shows the highest IQR and variance, with a mean similar to 2012 but higher than 2014. 2014 had maximum precipitation, the most extensive range. Temperature means across years were comparable, though 2013 exhibited more significant variance and IQR, indicating more dispersed middle values.

4.3.2. Comparative Analysis of Prediction Methods in Air Quality Data

We compare the proposed MMformer with three baseline models—Transformer, iTransformer, and SARIMAX—using MSE, MAE, and MAPE as primary evaluation metrics. the Transformer is considered a benchmark model in MTS forecasting [71] because its self-attention mechanism. iTransformer refines the Transformer architecture to enhance robustness and accuracy in MTS and achieves state-of-the-art performance in real-world scenarios [72]. SARIMAX (Seasonal Autoregressive Integrated Moving Average Model with Exogenous Variables) is a widely adopted statistical model that offers theoretical interpretability by incorporating seasonal and exogenous factors [73]. Including SARIMAX highlights the contrast between neural networks and traditional methods in complex, multivariate problems.

Table 6: Multivariate time series forecasting results using a real-world air quality dataset. Results are averaged across all prediction lengths (Avg). Figures in bold are the best for that metric

Model	MSE	MAE	MAPE
MMformer	0.53	0.48	26.53%
Transformer[57]	1.41	0.83	51.32%
iTransformer[21]	1.11	0.60	33.47%
SARIMAX[74]	215.17	6.90	10.86%

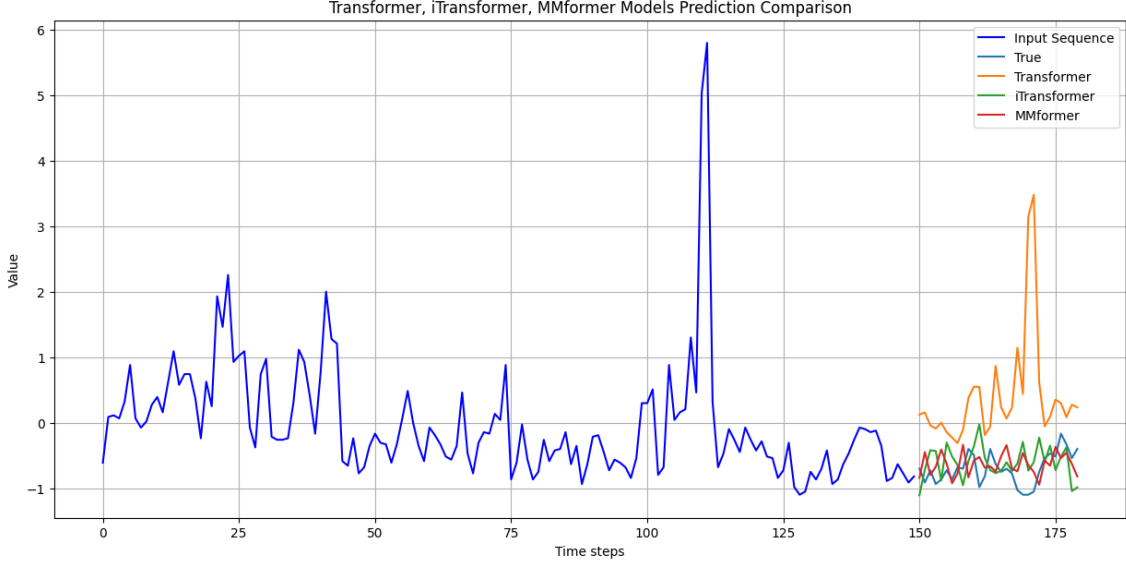


Figure 11: Models Prediction Comparison in Air Quality Data

Table 6 demonstrates that, despite using a high-performance system (Intel Core i9-12900KF CPU, 64GB RAM, RTX 3090 GPU), the three neural network models substantially outperform SARIMAX across most metrics, except for MAPE. This suggests that traditional time series models struggle with variability in multivariate data. In contrast, deep networks may sometimes over- or underestimate extreme values, inflating relative errors and thus MAPE. However, while SARIMAX can avoid large percentage deviations when trends are more obvious, its global accuracy—reflected by MSE and MAE—remains lower than that of the neural network approaches.

For data preparation, we allocated 730 days for training, 366 days for validation, and 181 days for testing, employing a sliding window strategy to capture temporal dependencies. Sequence lengths, prediction horizons, and hyperparameters were carefully aligned across all models to ensure a fair comparison.

Fig.11 compares all tested models except SARIMAX, which was excluded due to severe distortion that would hinder observation of other predictions. Although SARIMAX shows a respectable fit in Fig.12, it suffers from notable deviations at outlier points and abrupt changes, consistent with the inherent challenges that traditional methods face when modeling nonlinear structures. Fig.11 demonstrates MMformer’s overall advantage in capturing intrinsic properties of MTS data. Fig.16 – Fig.18 demonstrate each model’s predictions on the test dataset.

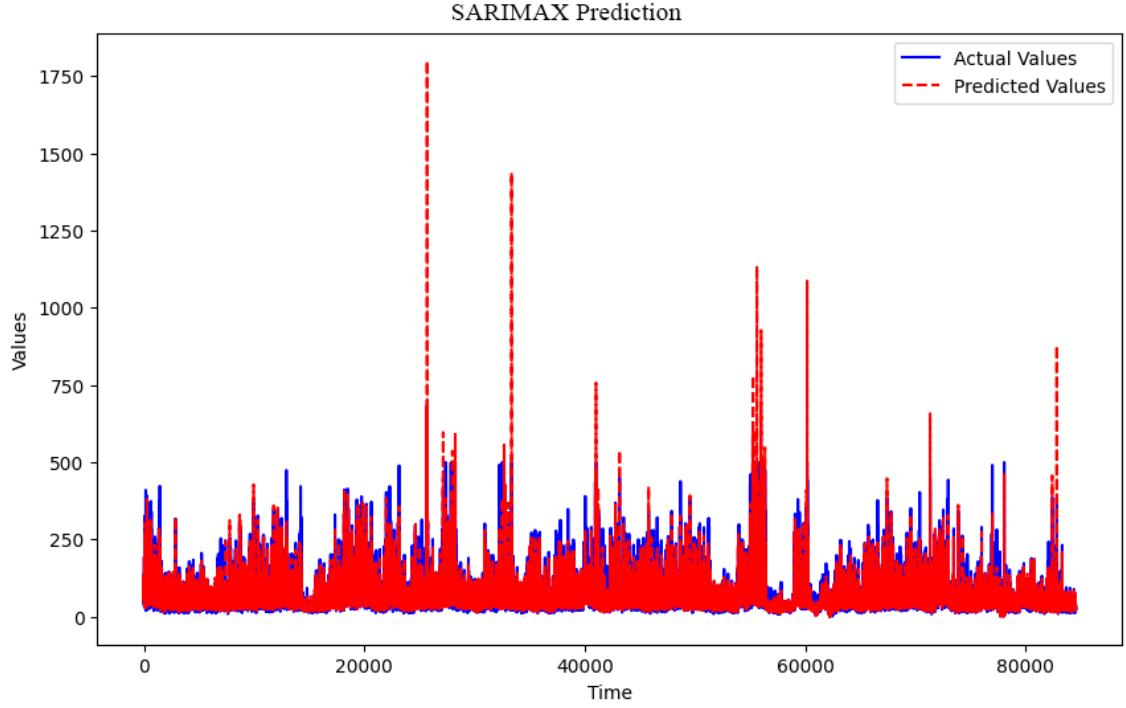


Figure 12: SARIMAX Prediction in Air Quality Test Dataset

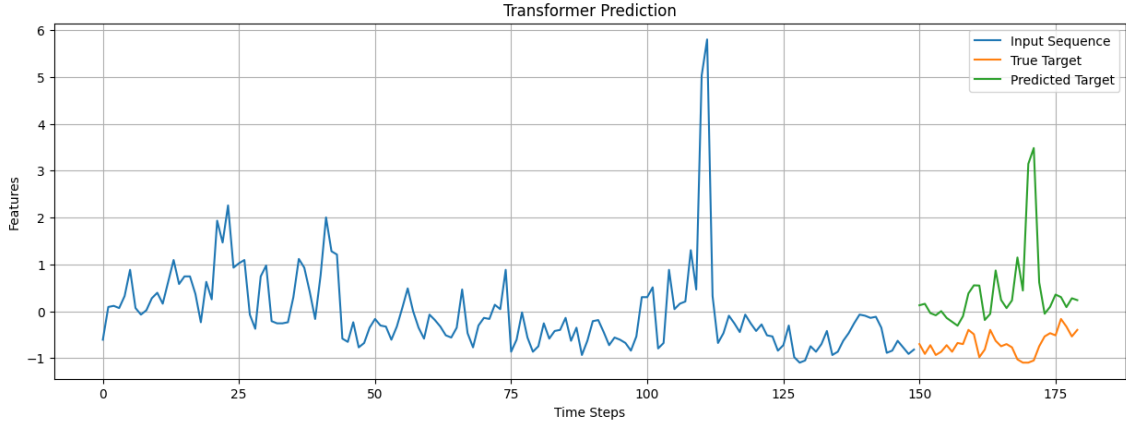


Figure 15: Transformer Prediction in Air Quality Test Dataset

We visualized the predictions for seven features on five test samples with the lowest MSE to further examine the models' performance. MMformer, as shown in Fig.16, can more closely track the ground truth, even in significant variability. This suggests MMformer's modeling structure and attention mechanisms more effectively capture global and local dependencies within the complex MTS.

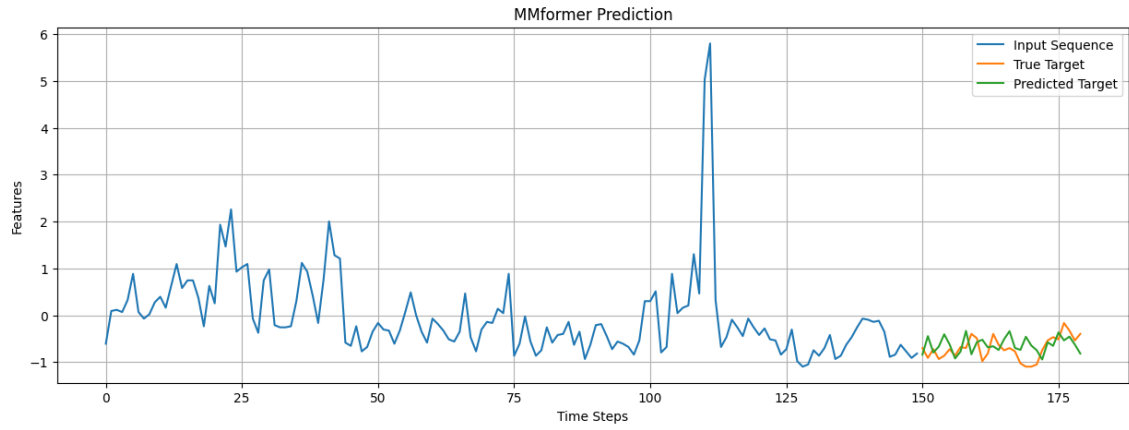


Figure 13: MMformer Prediction in Air Quality Test Dataset

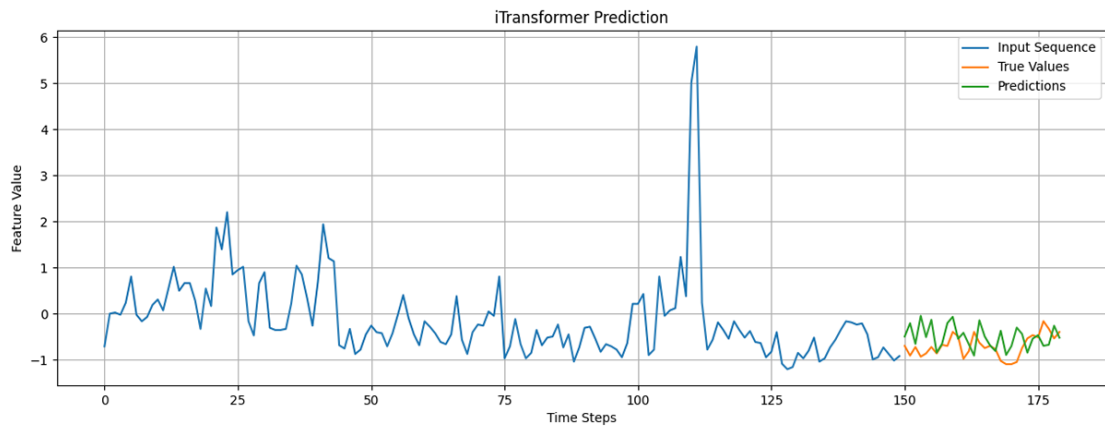


Figure 14: iTransformer Prediction in Air Quality Test Dataset



Figure 17: Transformer prediction in the test dataset with the five test samples with the lowest MSE in Air Quality

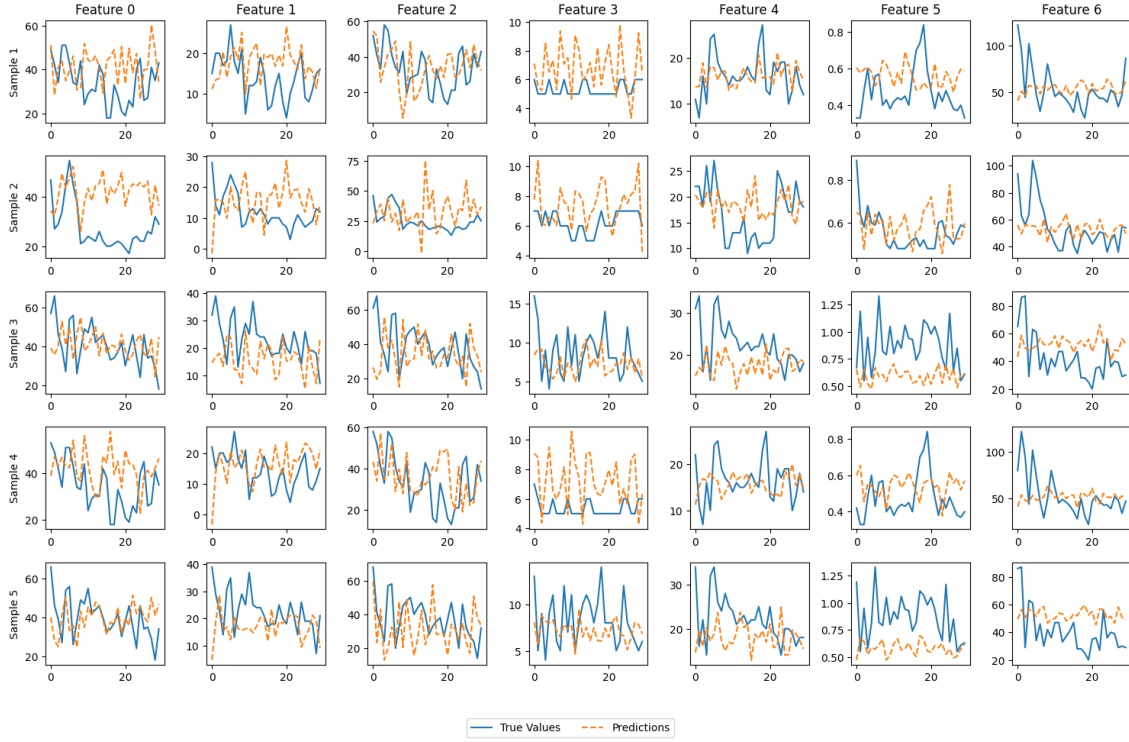


Figure 16: MMformer prediction in the test dataset with the five test samples with the lowest MSE in Air Quality

In contrast, Fig.17 exhibits Transformer significant deviations from the truth, particularly in regions with abrupt fluctuations or sharp peaks. This suggests that the Transformer’s self-attention may struggle to maintain accurate predictions during periods of high variability in MTS. Fig.18 demonstrates the challenges faced by the iTransformer model when dealing with rapid changes in the data, which illustrates how predictions become distorted under significant variability. For example, in several subplots, sudden peaks in the truth are smoothed or delayed in the predictions. This suggests that embedding timestamps alone may be insufficient to maintain sequence integrity across diverse regions and may introduce higher sensitivity to noise or regional variability.

In conclusion, our combined quantitative evaluation and systematic graphical analysis provide compelling evidence of the MMformer’s superior performance compared to the Transformer and iTransformer baselines. The observed shortcomings of the competing models in preserving critical patterns under adverse noise conditions further highlight the advantages of the proposed MMformer for modeling complex, multivariate time series.

4.3.3. Comparative Analysis of Prediction Methods in Climate Data

Similar to the previous methodology, the climate dataset MMformer will be compared with Transformer, iTransformer, and traditional SARIMAX models using identical evaluation metrics. The analysis will assess actual prediction results to provide a comprehensive performance overview.

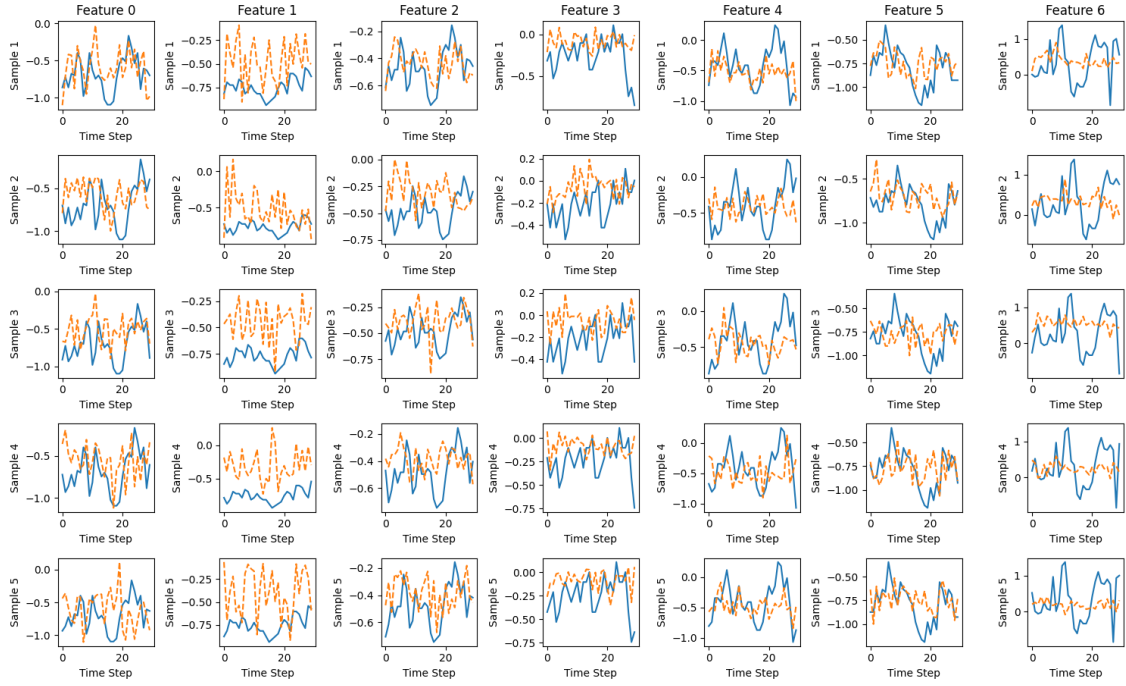


Figure 18: iTransformer prediction in the test dataset with the five test samples with the lowest MSE in Air Quality

Table 7: Multivariate time series forecasting results using a real-world climate dataset. Results are averaged across all prediction lengths (Avg). Figures in bold are the best for that metric

Model	MSE	MAE	MAPE
MMformer	0.68	0.45	25.30%
Transformer	1.10	0.65	38.42%
iTransformer	0.74	0.45	25.64%
SARIMAX	12201.06	41.08	96.86%

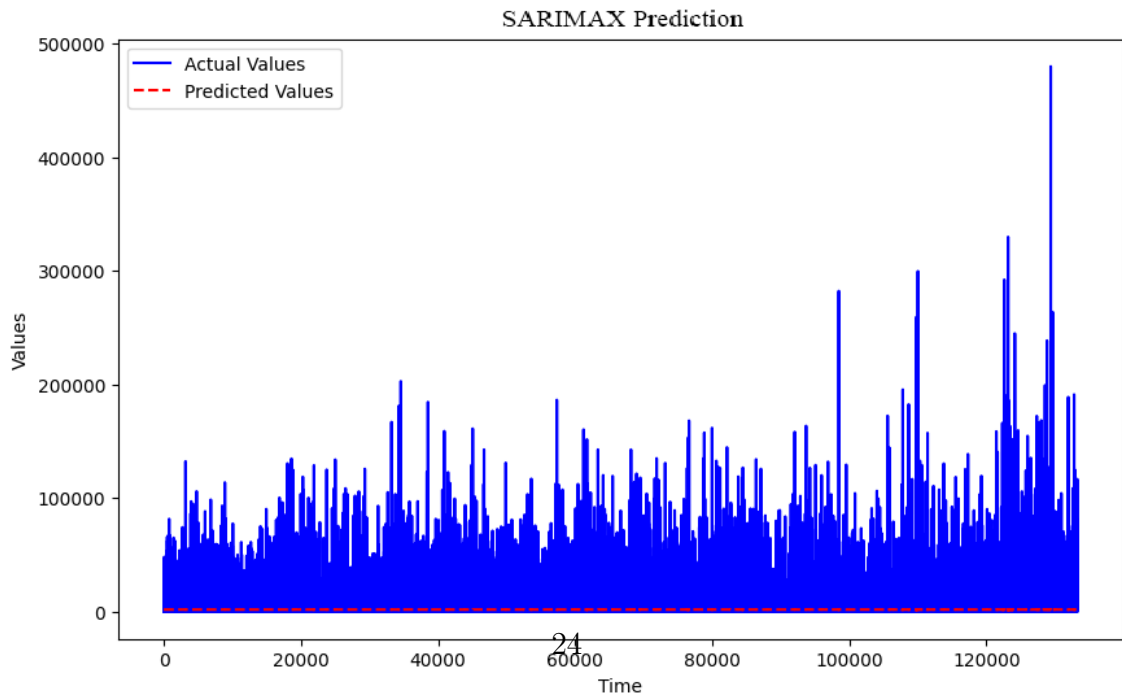


Figure 20: SARIMAX Prediction in Climate Test Dataset

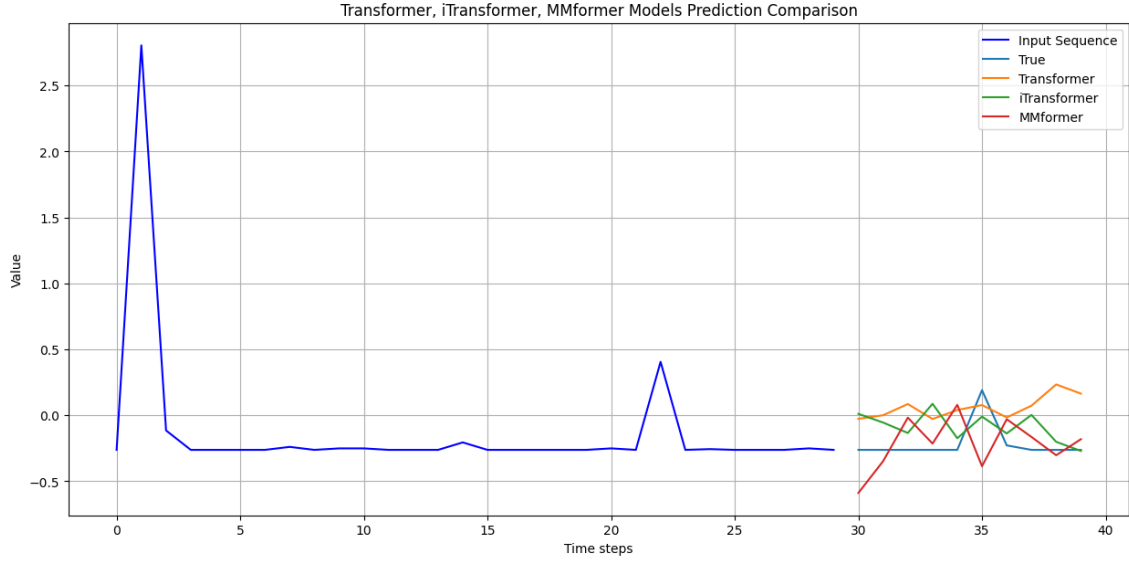


Figure 19: Models Prediction Comparison in Climate Data

Table 7 demonstrates that MMformer significantly outperforms other models when evaluated on comparable hardware, with all three neural network approaches substantially surpassing SARIMAX. This further confirms the limitations of traditional time series models. The dataset was partitioned into 160 days for training, 60 days for validation, and 56 days for testing, with sliding window techniques employed to maximize training data utilization. Sequence lengths and prediction horizons are the same across all models to ensure a fair comparison.

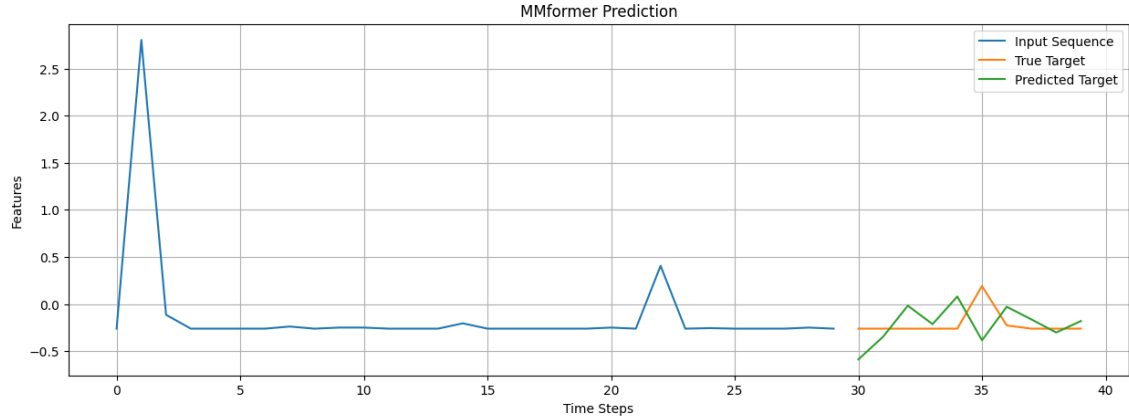


Figure 21: MMformer Prediction in Climate Test Dataset

Fig.20 demonstrates the limitations of the SARIMAX model, which significantly underperforms compared to the other methods across the entire time series. This poor performance on the dataset justifies the decision to exclude SARIMAX from the comparative analysis shown in Fig.19. The decline in SARIMAX performance when transitioning from air quality data to climate data can be attributed to fundamental characteristics of both the model and datasets. SARIMAX fundamentally depends on robustly identifying seasonal patterns and autoregressive relationships to generate

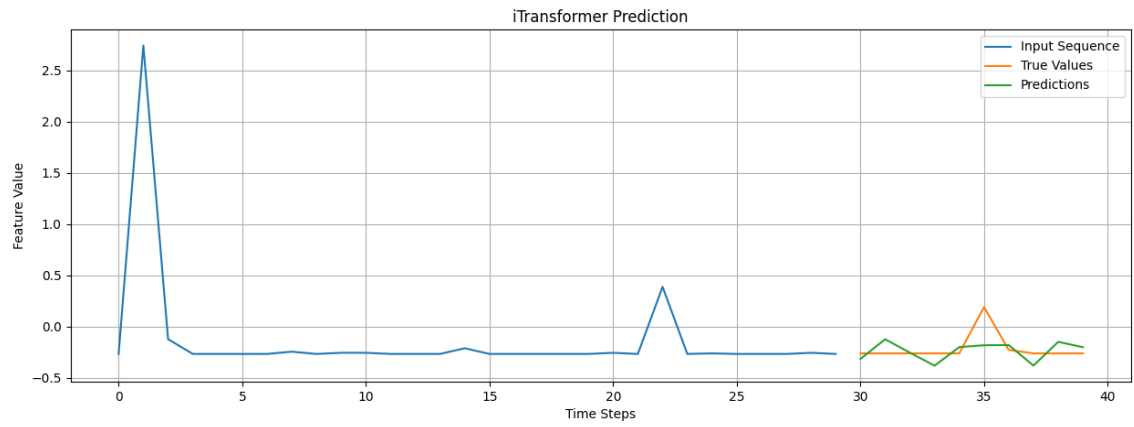


Figure 22: iTransformer Prediction in Climate Test Dataset

accurate forecasts.

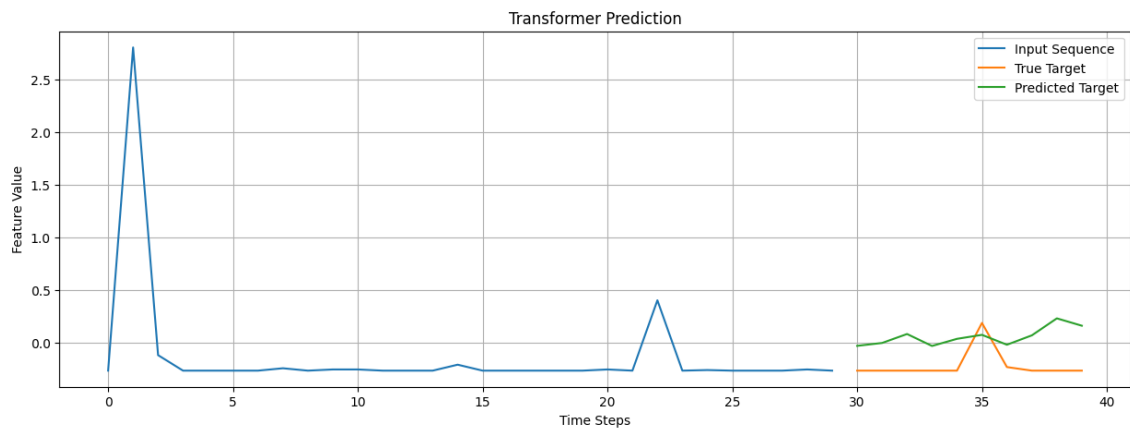


Figure 23: Transformer Prediction in Climate Test Dataset

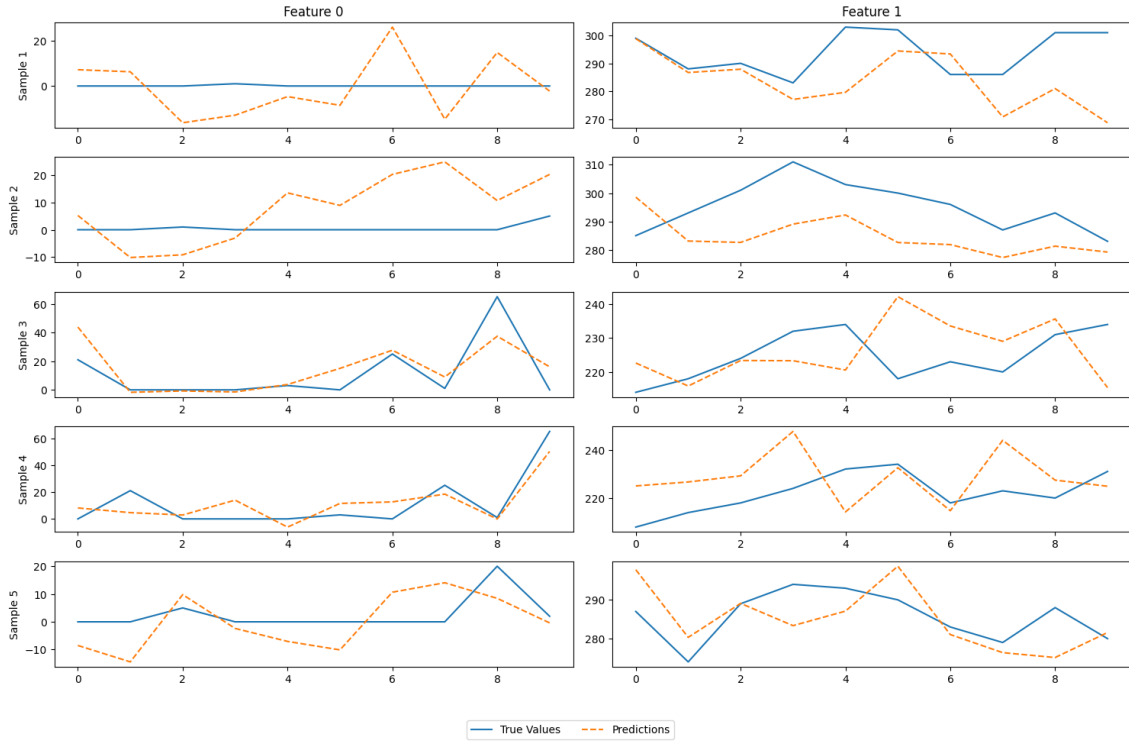


Figure 24: MMformer prediction in the test dataset with the five test samples with the lowest MSE in Climate Dataset

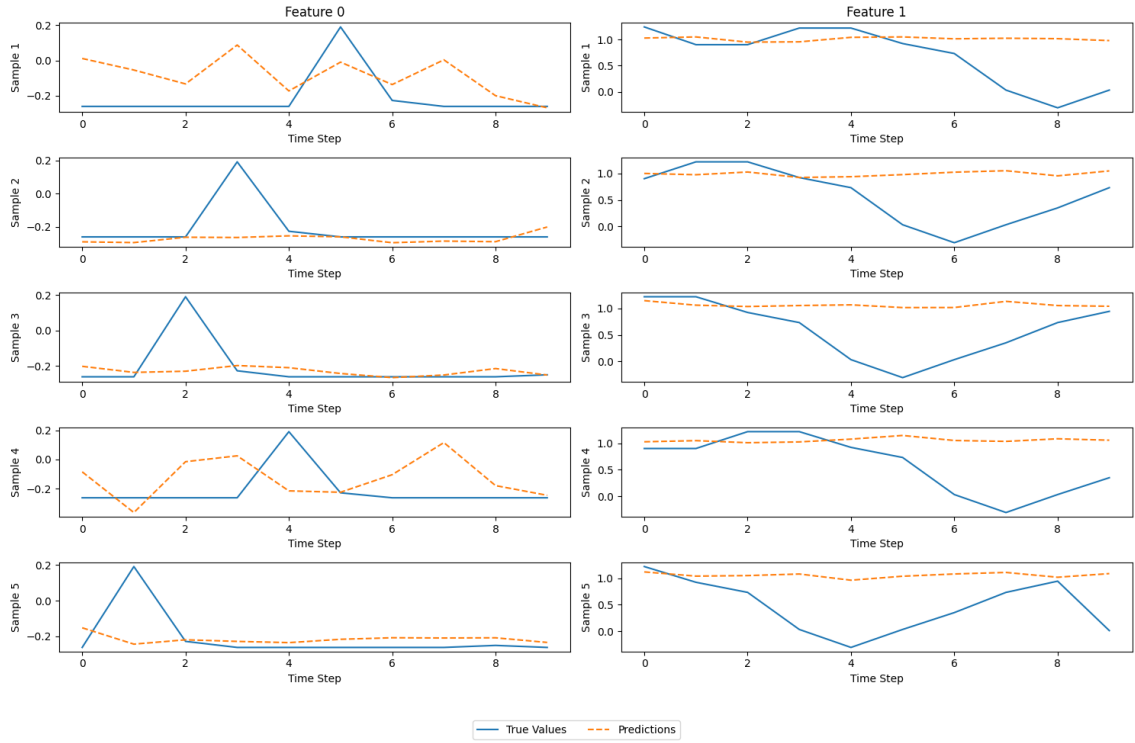


Figure 25: iTransformer prediction in the test dataset with the five test samples with the lowest MSE in Climate Dataset

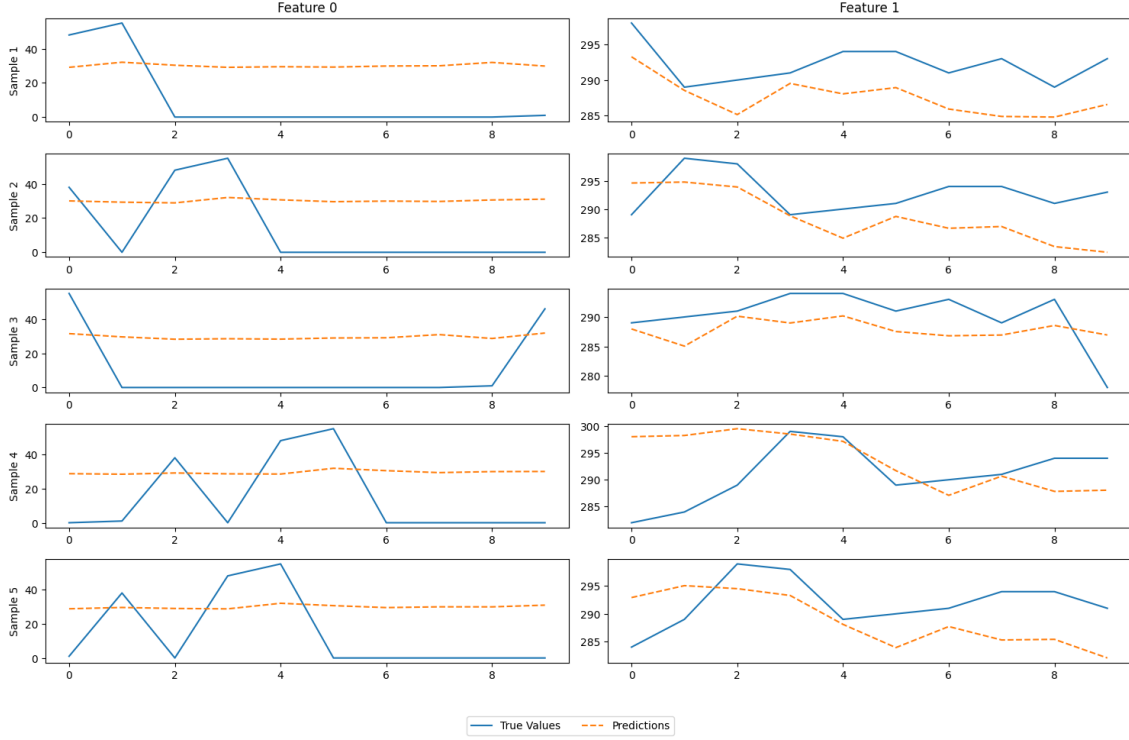


Figure 26: Transformer prediction in the test dataset with the five test samples with the lowest MSE in Climate Dataset

While the air quality dataset provides continuous observations over an extended timeframe (1277 days), the climate dataset contains only short temporal segments (276 days) of rainfall and temperature measurements collected exclusively during summer periods across three consecutive years. This temporal fragmentation disrupts the continuity necessary for effective seasonal pattern recognition. Furthermore, the substantially reduced time series length in the climate dataset compromises the statistical reliability of seasonal components and autoregressive relationships that SARIMAX relies upon for prediction accuracy.

The plots in Fig. 21 - 23 provide a detailed comparison of the model predictions against the actual target values for the test dataset. These figures illustrate the MMformer’s superior performance, which can closely track the fluctuations in the target variable over time. In contrast, Transformer and iTransformer exhibit more significant deviation from the actual values, particularly during periods of high volatility.

The consistent accuracy of MMformer’s predictions, as evidenced across these figures, supports the claim that it is the most effective MTS model for this application. The visual comparison of model outputs reinforces the quantitative metrics presented earlier, demonstrating MMformer’s superiority comprehensively over the other techniques evaluated.

We visualized the predictions of the two features from the five test samples with the lowest MSE to further evaluate each model’s performance (Fig.24–26). Fig.24 demonstrates that the MMformer model can accurately capture the overall trends and relationships between the features across the five test samples with the lowest MSE. The predicted values closely track the actual values, indicating that MMformer

can preserve the global dependencies between the features even when the dataset dimensionality is reduced.

In contrast, Fig.25 and Fig.26 reveal limitations in the ability of iTransformer and Transformer to model the local interactions between the two features jointly. While these models perform well on the reduced dataset according to the MSE metric in Table 7, the visualizations show that they struggle to capture the nuanced, localized patterns in the authentic feature relationships. The predicted values often deviate significantly from the ground truth, suggesting these models fail to preserve local dependencies when constrained to a fully constrained feature space.

By comparing the performance of the three models on these visualization plots, it is clear that the MMformer architecture is more effective at learning both the global trends and local interactions between features, even when the dataset dimensionality is greatly reduced. The quantitative metrics and visual analysis on the (331,1277,7) and (2415,276,2) datasets confirm that MMformer outperforms iTransformer, Transformer, and SARIMAX in modeling complex MTS relationships, demonstrating robust stability and generalization.

4.3.4. Ablation Study

To assess the contribution of each MMformer component, we conducted ablation experiments by removing the MAML and MC Dropout modules. We evaluated the models based on MSE, MAE, and MAPE using an air quality dataset.

Table 8: Ablation experiment results using a real-world air quality dataset. Results are averaged across all prediction lengths (Avg). Figures in bold are the best for that metric

Model	MSE	MAE	MAPE
MMformer	0.53	0.48	26.53%
Remove MAML	0.64	0.64	36.57%
Remove MC Dropout	0.57	0.52	29.08%
Remove MAMAL and MC Dropout	1.1	0.6	33.47%

Table 8 presents the comparative performance of the original MMformer, MMformer without meta-learning, MMformer without MC Dropout, and MMformer without both meta-learning and MC Dropout. While the corresponding values of MSE, MAE, and MAPE are relatively similar, it is evident that MMformer achieves the best overall performance, with the best values of MSE, MAE, and MAPE.

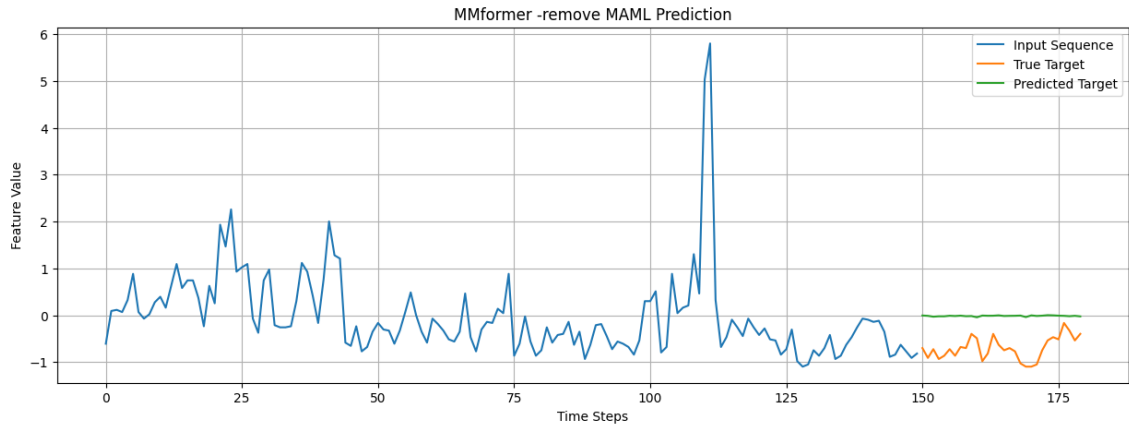


Figure 27: MMformer -remove MAML Prediction in Test Dataset

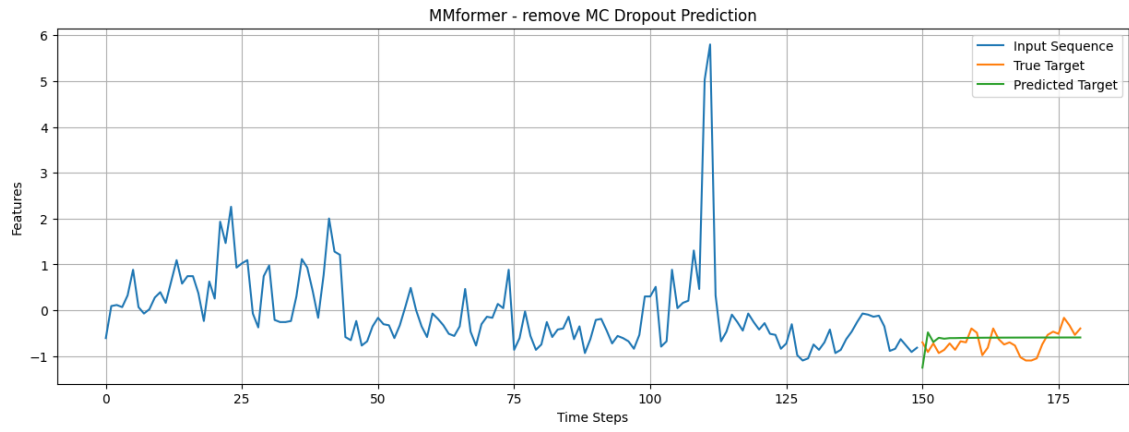


Figure 28: MMformer -remove MC Dropout Prediction in Test Dataset

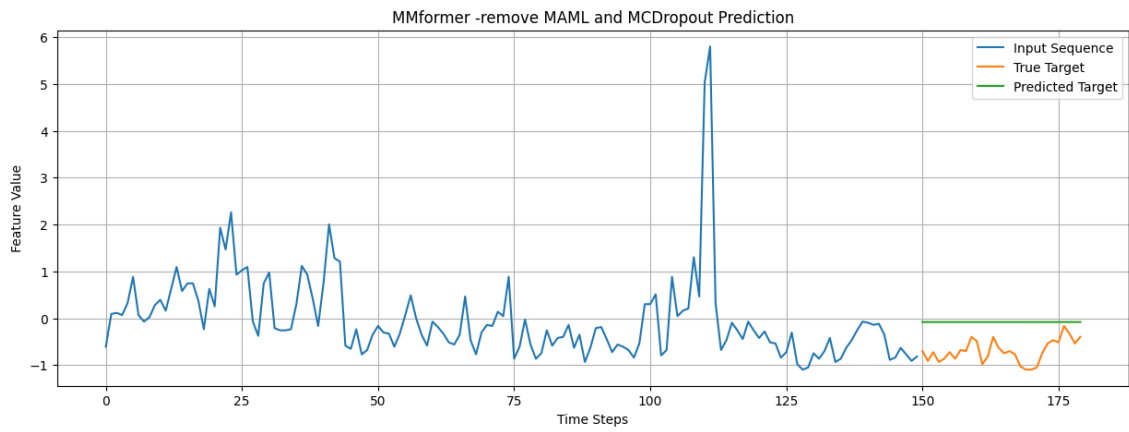


Figure 29: MMformer -remove MAML and MC Dropout Prediction in Test Dataset

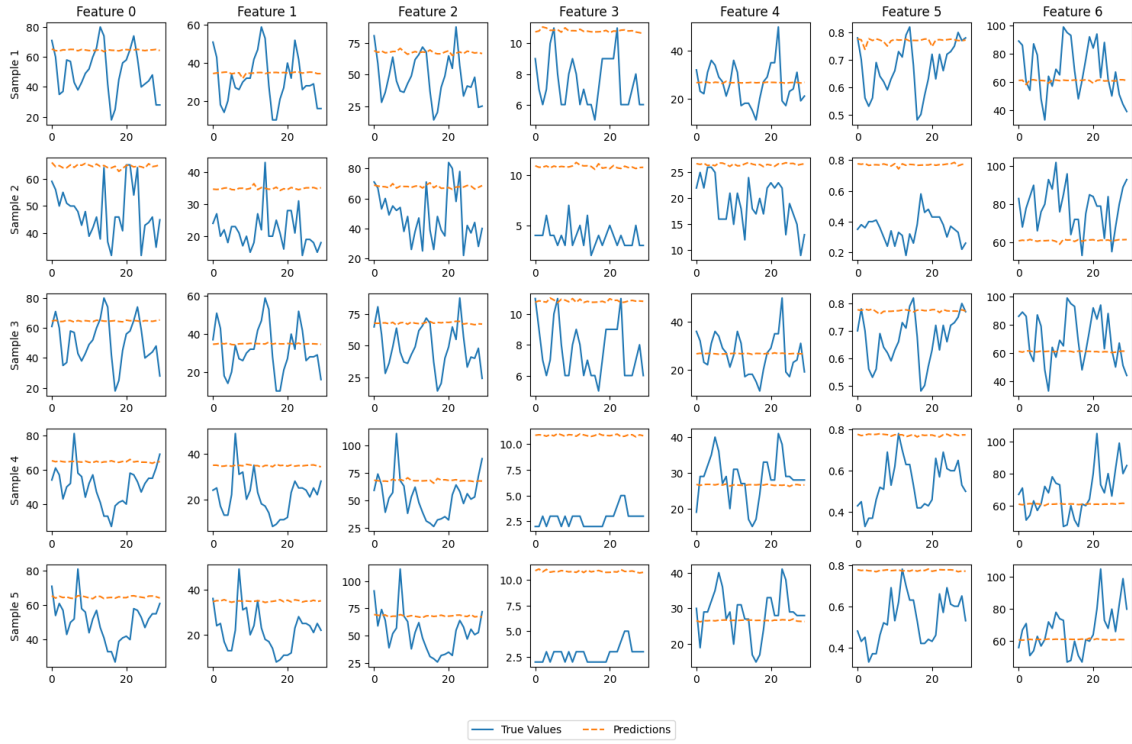


Figure 30: MMformer -remove MAML Prediction in Test Dataset with the 5 test samples with the lowest MSE

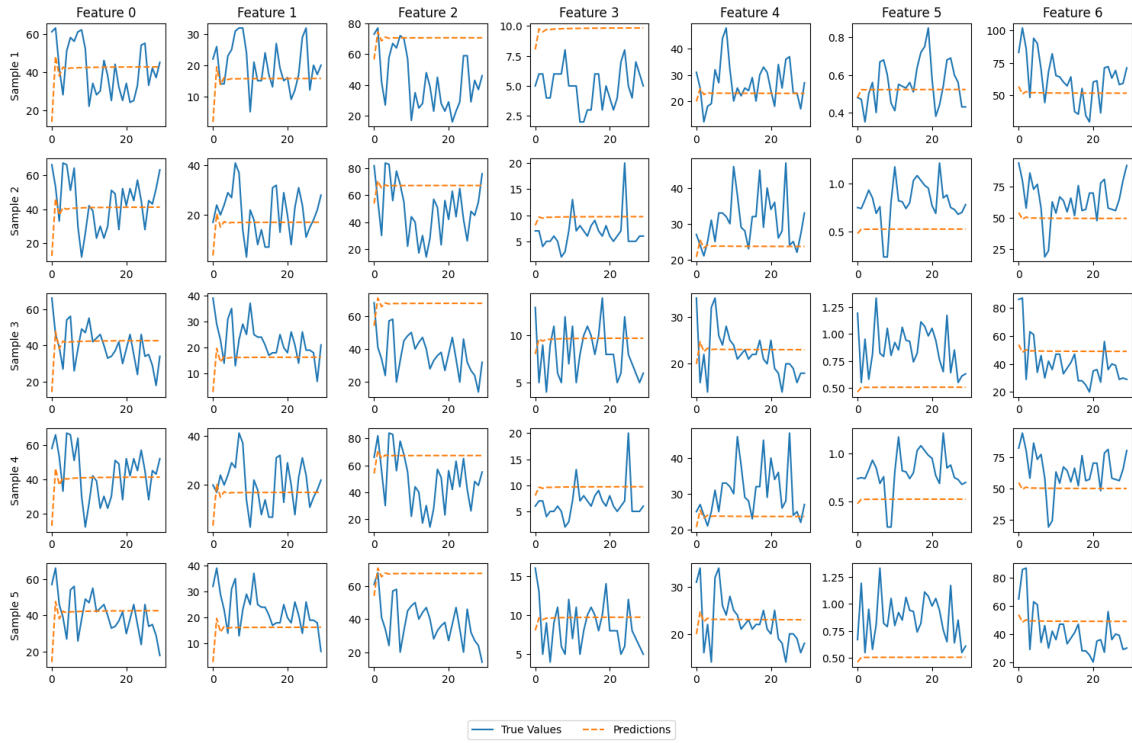


Figure 31: MMformer -remove MC Dropout Prediction in Test Dataset with the 5 test samples with the lowest MSE

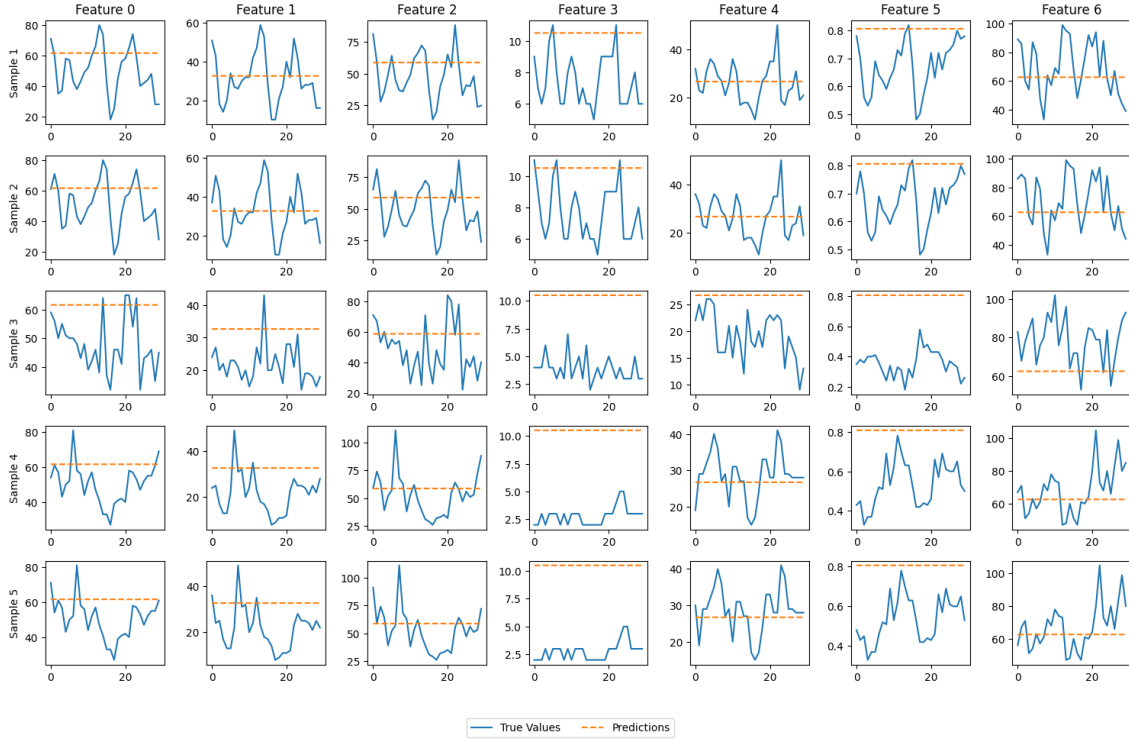


Figure 32: MMformer -remove MC Dropout Prediction in Test Dataset with the 5 test samples with the lowest MSE

Fig.13 and Fig.27-29 offer a more detailed visualization of the predicted trajectories under the various ablation settings. A direct comparison of those figures demonstrates that excluding MAML or MC Dropout leads to more pronounced deviations from the ground truth, particularly when abrupt changes occur in the time series. Specifically, excerpts where the data fluctuate rapidly highlight lagged or oversmoothed predictions for the ablated variants, whereas the complete MMformer maintains closer alignment with observed values.

Furthermore, analysis of the five test samples that exhibit the lowest MSE (Fig.30 - 32) reinforces this observation. In these figures, even minor discrepancies become apparent as the ablated models fail to accurately capture the subtler shifts in the data, indicating a reduction in robustness compared to the original MMformer. Likewise, direct comparisons between Fig.16 and Fig.30-32 (ablated versions) provide additional evidence that removing either MAML or MC Dropout compromises predictive stability and accuracy.

Ablation experiment evaluation quantitative outcomes (Table 8) and visual analysis demonstrate that both MAML and MC Dropout play a critical role in enhancing the MMformer’s capability to learn complex temporal dynamics, thereby ensuring consistent and robust performance in multivariate time-series forecasting. The model’s multi-layer linear structure and MAML further help avoid overfitting. Ablation experiments, which involved removing these modules, revealed notable decreases in prediction accuracy and robustness.

5. Conclusion and Future Work

This research focuses on developing a robust, high-accuracy framework for forecasting MTS. The proposed MMformer model integrates an adaptive, transferable multi-head attention mechanism with model-agnostic meta-learning (MAML) to extract and leverage underlying temporal-spatial patterns in MTS data effectively. By adaptively fine-tuning the encoder, whose parameters are transferred to the decoder, MMformer reduces the need for extensive manual parameter tuning and ensures reliable forecasts with minimal computational overhead. We assessed the performance of MMformer in forecasting MTS related to air quality and climate. Our findings indicate that MMformer provides accurate environmental change predictions with minimal computational overhead, outperforming iTransformer, Transformer, and the traditional SARIMAX model.

Despite MMformer’s notable strengths, such as its outperformance in extended-horizon forecasting, applicability across diverse regions, and capacity to handle multiple environmental factors, it still presents certain limitations. First, although the built-in MAML mechanism is generally effective for rapid adaptation in small-scale data scenarios, ensuring robust generalization across geographically expansive regions with markedly different data distributions often necessitates training on more diverse datasets. The reason is that substantial inter-regional variation demands richer samples to learn meta-representations that exhibit broad applicability. Second, although Bayesian approximate inference helps mitigate information loss, it invariably increases the complexity of the training process and diminishes transparency for non-technical stakeholders. These shortcomings underscore the importance of further research to bolster the model’s robustness and scalability.

Future work will address these shortcomings through (1) exploring semi-supervised or transfer learning approaches to reduce data requirements and enhance the model’s regional adaptability, (2) refining the approximate inference to improve computational efficiency and interpretability. These endeavors will further strengthen MMformer’s capability to detect and address environmental concerns at both local and global scales, ultimately contributing to more targeted interventions and enhanced resilience against the adverse effects of environmental changes.

In conclusion, MMformer is a robust, precise framework for MTS analysis. Future research should concentrate on scaling the model for broader datasets and exploring its potential in other domains with complex multivariate time series dynamics.

Declaration of Competing Interest

The authors declare that they have no known competing financial interests or personal relationships that could have appeared to influence the work reported in this article.

Acknowledgement

We sincerely thank the Climatic Data Centre, part of the National Meteorological Information Centre (CMA Meteorological Data Centre), for their invaluable assistance and cooperation in providing us with the meteorological data used in this study.

References

- [1] S. Li, T. Yao, W. Yang, W. Yu, M. Zhu, [Melt season hydrological characteristics of the parlung no. 4 glacier, in gangrigabu mountains, south-east tibetan plateau](#), *Hydrological Processes* 30 (8) (2016) 1171–1191. [arXiv:https://onlinelibrary.wiley.com/doi/pdf/10.1002/hyp.10696](#), [doi:https://doi.org/10.1002/hyp.10696](#).
URL [https://onlinelibrary.wiley.com/doi/abs/10.1002/hyp.10696](#)
- [2] H. Zhao, Y. Wang, J. Duan, C. Huang, D. Cao, Y. Tong, B. Xu, J. Bai, J. Tong, Q. Zhang, Multivariate time-series anomaly detection via graph attention network, in: 2020 IEEE International Conference on Data Mining (ICDM), 2020, pp. 841–850. [doi:10.1109/ICDM50108.2020.00093](#).
- [3] W. Xu, H. Peng, X. Zeng, F. Zhou, X. Tian, X. Peng, A hybrid modelling method for time series forecasting based on a linear regression model and deep learning, *Applied Intelligence* 49 (2019) 3002–3015.
- [4] M. Barandas, D. Folgado, L. Fernandes, S. Santos, M. Abreu, P. Bota, H. Liu, T. Schultz, H. Gamboa, Tsfel: Time series feature extraction library, *SoftwareX* 11 (2020) 100456.
- [5] Y. Zou, R. V. Donner, N. Marwan, J. F. Donges, J. Kurths, Complex network approaches to nonlinear time series analysis, *Physics Reports* 787 (2019) 1–97.
- [6] H. Hewamalage, C. Bergmeir, K. Bandara, Recurrent neural networks for time series forecasting: Current status and future directions, *International Journal of Forecasting* 37 (1) (2021) 388–427.
- [7] A. A. Ismail, M. Gunady, H. Corrada Bravo, S. Feizi, Benchmarking deep learning interpretability in time series predictions, *Advances in neural information processing systems* 33 (2020) 6441–6452.
- [8] W. Jiang, Applications of deep learning in stock market prediction: recent progress, *Expert Systems with Applications* 184 (2021) 115537.
- [9] R. Moskovitch, Multivariate temporal data analysis-a review, *Wiley Interdisciplinary Reviews: Data Mining and Knowledge Discovery* 12 (1) (2022) e1430.
- [10] E. Brophy, Z. Wang, Q. She, T. Ward, Generative adversarial networks in time series: A survey and taxonomy, *arXiv preprint arXiv:2107.11098* (2021).
- [11] S. Harford, F. Karim, H. Darabi, Generating adversarial samples on multivariate time series using variational autoencoders, *IEEE/CAA Journal of Automatica Sinica* 8 (9) (2021) 1523–1538. [doi:10.1109/JAS.2021.1004108](#).
- [12] S.-C. Wen, C.-H. Yang, [Time series analysis and prediction of nonlinear systems with ensemble learning framework applied to deep learning neural networks](#), *Information Sciences* 572 (2021) 167–181. [doi:https://doi.org/10.1016/j.ins.2021.04.094](#).

URL <https://www.sciencedirect.com/science/article/pii/S0020025521004357>

- [13] S. Jiang, R. Xiao, L. Wang, X. Luo, C. Huang, J.-H. Wang, K.-S. Chin, X. Nie, Combining deep neural networks and classical time series regression models for forecasting patient flows in hong kong, *IEEE Access* 7 (2019) 118965–118974. [doi:10.1109/ACCESS.2019.2936550](https://doi.org/10.1109/ACCESS.2019.2936550).
- [14] P. Manigandan, M. S. Alam, M. Alharthi, U. Khan, K. Alagirisamy, D. Pachiyappan, A. Rehman, [Forecasting natural gas production and consumption in united states-evidence from sarima and sarimax models](#), *Energies* 14 (19) (2021). [doi:10.3390/en14196021](https://doi.org/10.3390/en14196021).
URL <https://www.mdpi.com/1996-1073/14/19/6021>
- [15] C. Nichiforov, I. Stamatescu, I. Făgărășan, G. Stamatescu, Energy consumption forecasting using arima and neural network models, in: 2017 5th International Symposium on Electrical and Electronics Engineering (ISEEE), 2017, pp. 1–4. [doi:10.1109/ISEEE.2017.8170657](https://doi.org/10.1109/ISEEE.2017.8170657).
- [16] C. Bentéjac, A. Csörgő, G. Martínez-Muñoz, [A comparative analysis of gradient boosting algorithms](#), *Artificial Intelligence Review* 54 (3) (2021) 1937–1967. [doi:10.1007/s10462-020-09896-5](https://doi.org/10.1007/s10462-020-09896-5).
URL <https://doi.org/10.1007/s10462-020-09896-5>
- [17] M. Schonlau, R. Y. Zou, [The random forest algorithm for statistical learning](#), *The Stata Journal* 20 (1) (2020) 3–29. [arXiv:https://doi.org/10.1177/1536867X20909688](https://arxiv.org/abs/https://doi.org/10.1177/1536867X20909688), [doi:10.1177/1536867X20909688](https://doi.org/10.1177/1536867X20909688).
URL <https://doi.org/10.1177/1536867X20909688>
- [18] D. A. Pisner, D. M. Schnyer, [Chapter 6 - Support vector machine](#), in: A. Mechelli, S. Vieira (Eds.), *Machine Learning*, Academic Press, 2020, pp. 101–121. [doi:https://doi.org/10.1016/B978-0-12-815739-8.00006-7](https://doi.org/10.1016/B978-0-12-815739-8.00006-7).
URL <https://www.sciencedirect.com/science/article/pii/B9780128157398000067>
- [19] B. K. Iwana, S. Uchida, [An empirical survey of data augmentation for time series classification with neural networks](#), *PLOS ONE* 16 (7) (2021) 1–32. [doi:10.1371/journal.pone.0254841](https://doi.org/10.1371/journal.pone.0254841).
URL <https://doi.org/10.1371/journal.pone.0254841>
- [20] W. Samek, G. Montavon, S. Lapuschkin, C. J. Anders, K.-R. Müller, Explaining deep neural networks and beyond: A review of methods and applications, *Proceedings of the IEEE* 109 (3) (2021) 247–278. [doi:10.1109/JPR0C.2021.3060483](https://doi.org/10.1109/JPR0C.2021.3060483).
- [21] Y. Liu, T. Hu, H. Zhang, H. Wu, S. Wang, L. Ma, M. Long, itransformer: Inverted transformers are effective for time series forecasting (2023). [arXiv:2310.06625](https://arxiv.org/abs/2310.06625).

- [22] T. Sharma, T. Reps, [A new abstraction framework for affine transformers](#), *Formal Methods in System Design* 54 (1) (2019) 110–143. doi:[10.1007/s10703-018-0325-z](https://doi.org/10.1007/s10703-018-0325-z).
URL <https://doi.org/10.1007/s10703-018-0325-z>
- [23] M.-H. Laves, S. Ihler, K.-P. Kortmann, T. Ortmaier, [Well-calibrated model uncertainty with temperature scaling for dropout variational inference](#) (2019). [arXiv:1909.13550](https://arxiv.org/abs/1909.13550).
- [24] G. Li, T. Meng, M. Li, M. Zhou, D. Han, [A dynamic short cascade diffusion prediction network based on meta-learning-transformer](#), *Electronics* 12 (4) (2023). doi:[10.3390/electronics12040837](https://doi.org/10.3390/electronics12040837).
URL <https://www.mdpi.com/2079-9292/12/4/837>
- [25] S. A. Horn, P. K. Dasgupta, [The Air Quality Index \(AQI\) in historical and analytical perspective a tutorial review](#), *Talanta* 267 (2024) 125260. doi:<https://doi.org/10.1016/j.talanta.2023.125260>.
URL <https://www.sciencedirect.com/science/article/pii/S0039914023010111>
- [26] A. Benchrif, A. Wheida, M. Tahri, R. M. Shubbar, B. Biswas, [Air quality during three covid-19 lockdown phases: AQI, PM2.5 and NO2 assessment in cities with more than 1 million inhabitants](#), *Sustainable Cities and Society* 74 (2021) 103170. doi:<https://doi.org/10.1016/j.scs.2021.103170>.
URL <https://www.sciencedirect.com/science/article/pii/S2210670721004510>
- [27] China Meteorological Data Service Centre, [Historical dataset of surface meteorological observations in china](#), China Meteorological Data Service Centre-National Meteorological Information Center (2023).
URL <https://www.cnemc.cn/sssj/>
- [28] G. Zerveas, S. Jayaraman, D. Patel, A. Bhamidipaty, C. Eickhoff, [A transformer-based framework for multivariate time series representation learning](#), in: *Proceedings of the 27th ACM SIGKDD Conference on Knowledge Discovery & Data Mining, KDD '21*, Association for Computing Machinery, New York, NY, USA, 2021, p. 2114–2124. doi:[10.1145/3447548.3467401](https://doi.org/10.1145/3447548.3467401).
URL <https://doi.org/10.1145/3447548.3467401>
- [29] Y. Hu, F. Xiao, [Network self attention for forecasting time series](#), *Applied Soft Computing* 124 (2022) 109092. doi:<https://doi.org/10.1016/j.asoc.2022.109092>.
URL <https://www.sciencedirect.com/science/article/pii/S1568494622003775>
- [30] A. Y. Yıldız, E. Koç, A. Koç, [Multivariate time series imputation with transformers](#), *IEEE Signal Processing Letters* 29 (2022) 2517–2521. doi:[10.1109/LSP.2022.3224880](https://doi.org/10.1109/LSP.2022.3224880).

- [31] S. Kim, E. Chung, P. Kang, [FEAT: A general framework for feature-aware multivariate time-series representation learning](#), Knowledge-Based Systems 277 (2023) 110790. doi:<https://doi.org/10.1016/j.knosys.2023.110790>. URL <https://www.sciencedirect.com/science/article/pii/S0950705123005403>
- [32] N. M. Foumani, C. W. Tan, G. I. Webb, M. Salehi, [Improving position encoding of transformers for multivariate time series classification](#), Data Mining and Knowledge Discovery (Sep. 2023). doi:[10.1007/s10618-023-00948-2](https://doi.org/10.1007/s10618-023-00948-2). URL <https://doi.org/10.1007/s10618-023-00948-2>
- [33] S. Makridakis, E. Spiliotis, V. Assimakopoulos, [Statistical and Machine Learning forecasting methods: Concerns and ways forward](#), PLOS ONE 13 (3) (2018) 1–26, publisher: Public Library of Science. doi:[10.1371/journal.pone.0194889](https://doi.org/10.1371/journal.pone.0194889). URL <https://doi.org/10.1371/journal.pone.0194889>
- [34] R. E. Caraka, S. Abu Bakar, M. Tahmid, Rainfall forecasting multi kernel support vector regression seasonal autoregressive integrated moving average (mksvr-sarima), in: M. Latif, N. Ibrahim, M. Hanafiah, S. Hasbullah, M. Jumali, K. Ibrahim, N. Rasol (Eds.), 2018 UKM FST POSTGRADUATE COLLOQUIUM, Vol. 2111 of AIP Conference Proceedings, 2019, postgraduate Colloquium of the Faculty-of-Science-and-Technology of the Universiti-Kebangsaan-Malaysia (UKM FST), Univ Kebangsaan Malaysia, Fac Sci & Technol, Selangor, MALAYSIA, APR 04-06, 2018. doi:[10.1063/1.5111221](https://doi.org/10.1063/1.5111221).
- [35] Z. Liu, Z. Zhu, J. Gao, C. Xu, Forecast methods for time series data: A survey, IEEE Access 9 (2021) 91896–91912. doi:[10.1109/ACCESS.2021.3091162](https://doi.org/10.1109/ACCESS.2021.3091162).
- [36] A. Kaushal, A. K. Gupta, V. K. Sehgal, Exploiting the synergy of sarima and xgboost for spatiotemporal earthquake time series forecasting, EARTH SURFACE PROCESSES AND LANDFORMS (2024 OCT 1 2024). doi:[10.1002/esp.5992](https://doi.org/10.1002/esp.5992).
- [37] C.-C. SHEN, C.-K. WU, Y.-H. CHEN, J.-X. WANG, M.-H. YANG, H. ZHANG, [Advance in Novel Methods for Enrichment and Precise Analysis of Circulating Tumor Cells](#), Chinese Journal of Analytical Chemistry 49 (4) (2021) 483–495. doi:[https://doi.org/10.1016/S1872-2040\(21\)60089-0](https://doi.org/10.1016/S1872-2040(21)60089-0). URL <https://www.sciencedirect.com/science/article/pii/S1872204021600890>
- [38] Z. Hajirahimi, M. Khashei, Hybrid structures in time series modeling and forecasting: A review, ENGINEERING APPLICATIONS OF ARTIFICIAL INTELLIGENCE 86 (2019) 83–106. doi:[10.1016/j.engappai.2019.08.018](https://doi.org/10.1016/j.engappai.2019.08.018).
- [39] D. L. Marino, K. Amarasinghe, M. Manic, Building energy load forecasting using deep neural networks, in: IECON 2016 - 42nd Annual Conference of the IEEE Industrial Electronics Society, 2016, pp. 7046–7051. doi:[10.1109/IECON.2016.7793413](https://doi.org/10.1109/IECON.2016.7793413).

- [40] W. B. Nicholson, I. Wilms, J. Bien, D. S. Matteson, High dimensional forecasting via interpretable vector autoregression, *JOURNAL OF MACHINE LEARNING RESEARCH* 21 (2020).
- [41] R. Cai, Z. Lin, W. Chen, Z. Hao, Shared state space model for background information extraction and time series prediction, *NEUROCOMPUTING* 468 (2022) 85–96. [doi:10.1016/j.neucom.2021.10.010](https://doi.org/10.1016/j.neucom.2021.10.010).
- [42] S. M. Shaarawy, Bayesian modeling and forecasting of vector autoregressive moving average processes, *COMMUNICATIONS IN STATISTICS-THEORY AND METHODS* 52 (11) (2023) 3795–3815. [doi:10.1080/03610926.2021.1980047](https://doi.org/10.1080/03610926.2021.1980047).
- [43] W. B. Nicholson, I. Wilms, J. Bien, D. S. Matteson, High dimensional forecasting via interpretable vector autoregression, *Journal of Machine Learning Research* 21 (166) (2020) 1–52.
- [44] K. Kim, N. Sibanda, R. Arnold, T. A’mar, Enhancing data-limited assessments with random effects: a case study on korea chub mackerel (*scomber japonicus*), *CANADIAN JOURNAL OF FISHERIES AND AQUATIC SCIENCES* 81 (10) (2024) 1433–1455. [doi:10.1139/cjfas-2023-0358](https://doi.org/10.1139/cjfas-2023-0358).
- [45] M. Bansal, A. Goyal, A. Choudhary, A comparative analysis of k-nearest neighbor, genetic, support vector machine, decision tree, and long short term memory algorithms in machine learning, *Decision Analytics Journal* 3 (2022) 100071.
- [46] F. Arias del Campo, M. C. Guevara Neri, O. O. Vergara Villegas, V. G. Cruz Sanchez, H. d. J. Ochoa Dominguez, V. Garcia Jimenez, Auto-adaptive multilayer perceptron for univariate time series classification, *EXPERT SYSTEMS WITH APPLICATIONS* 181 (NOV 1 2021). [doi:10.1016/j.eswa.2021.115147](https://doi.org/10.1016/j.eswa.2021.115147).
- [47] P. H. M. Albuquerque, Y. Peng, J. P. F. d. Silva, Making the whole greater than the sum of its parts: A literature review of ensemble methods for financial time series forecasting, *JOURNAL OF FORECASTING* 41 (8) (2022) 1701–1724. [doi:10.1002/for.2894](https://doi.org/10.1002/for.2894).
- [48] H. Bi, L. Lu, Y. Meng, Hierarchical attention network for multivariate time series long-term forecasting, *Applied Intelligence* 53 (5) (2023) 5060–5071.
- [49] B. Lim, S. Zohren, [Time-series forecasting with deep learning: a survey](https://doi.org/10.1098/rsta.2020.0209), *Philosophical Transactions of the Royal Society A: Mathematical, Physical and Engineering Sciences* 379 (2194) (2021) 20200209. [doi:10.1098/rsta.2020.0209](https://doi.org/10.1098/rsta.2020.0209). URL <http://dx.doi.org/10.1098/rsta.2020.0209>
- [50] K. Bandara, C. Bergmeir, H. Hewamalage, Lstm-msnet: Leveraging forecasts on sets of related time series with multiple seasonal patterns, *IEEE Transactions on Neural Networks and Learning Systems* 32 (4) (2021) 1586–1599. [doi:10.1109/TNNLS.2020.2985720](https://doi.org/10.1109/TNNLS.2020.2985720).

- [51] A. Kamilaris, F. X. Prenafeta-Boldú, [Deep learning in agriculture: A survey](#), *Computers and Electronics in Agriculture* 147 (2018) 70–90. doi:<https://doi.org/10.1016/j.compag.2018.02.016>.
URL <https://www.sciencedirect.com/science/article/pii/S0168169917308803>
- [52] Z. Zhao, Bin Liang, X. Wang, W. Lu, [Remaining useful life prediction of aircraft engine based on degradation pattern learning](#), *Reliability Engineering & System Safety* 164 (2017) 74–83. doi:<https://doi.org/10.1016/j.ress.2017.02.007>.
URL <https://www.sciencedirect.com/science/article/pii/S0951832017302454>
- [53] S. Zargar, Introduction to sequence learning models: Rnn, lstm, gru, Department of Mechanical and Aerospace Engineering, North Carolina State University (2021).
- [54] S. M. Al-Selwi, M. F. Hassan, S. J. Abdulkadir, A. Muneer, Lstm inefficiency in long-term dependencies regression problems, *Journal of Advanced Research in Applied Sciences and Engineering Technology* 30 (3) (2023) 16–31.
- [55] X. Gonzalez, A. Warrington, J. T. Smith, S. W. Linderman, Towards scalable and stable parallelization of nonlinear rnns, *arXiv preprint arXiv:2407.19115* (2024).
- [56] X. Zhang, W. Jiang, J. Hu, Achieving full parallelism in lstm via a unified accelerator design, in: *2020 IEEE 38th International Conference on Computer Design (ICCD)*, IEEE, 2020, pp. 469–477.
- [57] Q. Wen, T. Zhou, C. Zhang, W. Chen, Z. Ma, J. Yan, L. Sun, [Transformers in time series: A survey](#), *International Joint Conferences on Artificial Intelligence Organization*, 2023, pp. 6778–6786, survey Track. doi:[10.24963/ijcai.2023/759](https://doi.org/10.24963/ijcai.2023/759).
URL <https://doi.org/10.24963/ijcai.2023/759>
- [58] H. Zhang, Y. Zou, X. Yang, H. Yang, A temporal fusion transformer for short-term freeway traffic speed multistep prediction, *Neurocomputing* 500 (2022) 329–340.
- [59] H. Zhou, S. Zhang, J. Peng, S. Zhang, J. Li, H. Xiong, W. Zhang, Informer: Beyond efficient transformer for long sequence time-series forecasting, in: *Proceedings of the AAAI conference on artificial intelligence*, Vol. 35, 2021, pp. 11106–11115.
- [60] G. Li, B. Choi, J. Xu, S. S Bhowmick, K.-P. Chun, G. L.-H. Wong, [ShapeNet: A Shapelet-Neural Network Approach for Multivariate Time Series Classification](#), *Proceedings of the AAAI Conference on Artificial Intelligence* 35 (9) (2021) 8375–8383. doi:[10.1609/aaai.v35i9.17018](https://doi.org/10.1609/aaai.v35i9.17018).
URL <https://ojs.aaai.org/index.php/AAAI/article/view/17018>

- [61] W. Shi, M. Zhang, R. Zhang, S. Chen, Z. Zhan, [Change detection based on artificial intelligence: State-of-the-art and challenges](#), Remote Sensing 12 (10) (2020). doi:[10.3390/rs12101688](https://doi.org/10.3390/rs12101688).
URL <https://www.mdpi.com/2072-4292/12/10/1688>
- [62] D. Cheng, F. Yang, S. Xiang, J. Liu, [Financial time series forecasting with multi-modality graph neural network](#), Pattern Recognition 121 (2022) 108218. doi:<https://doi.org/10.1016/j.patcog.2021.108218>.
URL <https://www.sciencedirect.com/science/article/pii/S003132032100399X>
- [63] J. Gao, X. Song, Q. Wen, P. Wang, L. Sun, H. Xu, Robusttad: Robust time series anomaly detection via decomposition and convolutional neural networks, arXiv preprint arXiv:2002.09545 (2020).
- [64] S.-Y. Shih, F.-K. Sun, H.-y. Lee, [Temporal pattern attention for multivariate time series forecasting](#), Machine Learning 108 (8) (2019) 1421–1441. doi:[10.1007/s10994-019-05815-0](https://doi.org/10.1007/s10994-019-05815-0).
URL <https://doi.org/10.1007/s10994-019-05815-0>
- [65] C. H. Lubba, S. S. Sethi, P. Knaute, S. R. Schultz, B. D. Fulcher, N. S. Jones, [catch22: CAnonical Time-series CHaracteristics](#), Data Mining and Knowledge Discovery 33 (6) (2019) 1821–1852. doi:[10.1007/s10618-019-00647-x](https://doi.org/10.1007/s10618-019-00647-x).
URL <https://doi.org/10.1007/s10618-019-00647-x>
- [66] C. Lemke, B. Gabrys, [Meta-learning for time series forecasting and forecast combination](#), Neurocomputing 73 (10) (2010) 2006–2016. doi:<https://doi.org/10.1016/j.neucom.2009.09.020>.
URL <https://www.sciencedirect.com/science/article/pii/S0925231210001074>
- [67] F. Xiao, L. Liu, J. Han, D. Guo, S. Wang, H. Cui, T. Peng, Meta-learning for few-shot time series forecasting, Journal of Intelligent & Fuzzy Systems 43 (1) (2022) 325–341, publisher: IOS Press. doi:[10.3233/JIFS-212228](https://doi.org/10.3233/JIFS-212228).
- [68] A. Vaswani, N. Shazeer, N. Parmar, J. Uszkoreit, L. Jones, A. N. Gomez, L. Kaiser, I. Polosukhin, Attention is all you need (2023). arXiv:[1706.03762](https://arxiv.org/abs/1706.03762).
- [69] D. S. K. Karunasingha, [Root mean square error or mean absolute error? use their ratio as well](#), Information Sciences 585 (2022) 609–629. doi:<https://doi.org/10.1016/j.ins.2021.11.036>.
URL <https://www.sciencedirect.com/science/article/pii/S0020025521011567>
- [70] S. Efendi, M. K. Nasution, M. Herman, et al., The role of detection rate in mape to improve measurement accuracy for predicting fintech data in various regressions, in: 2023 International Conference on Computer Science, Information Technology and Engineering (ICCoSITE), IEEE, 2023, pp. 874–879.

- [71] K. Mendis, M. Wickramasinghe, P. Marasinghe, Multivariate time series forecasting: A review, in: Proceedings of the 2024 2nd Asia Conference on Computer Vision, Image Processing and Pattern Recognition, 2024, pp. 1–9.
- [72] Y. Liu, T. Hu, H. Zhang, H. Wu, S. Wang, L. Ma, M. Long, [itransformer: Inverted transformers are effective for time series forecasting](#), in: The Twelfth International Conference on Learning Representations, 2024.
URL <https://openreview.net/forum?id=JePfAI8fah>
- [73] F. R. Alharbi, D. Csala, A seasonal autoregressive integrated moving average with exogenous factors (sarimax) forecasting model-based time series approach, *Inventions* 7 (4) (2022) 94.
- [74] K. Vivek, A. R. Deepti, F. Basith, Forecasting the consumer price index using sarimax modeling, in: 2024 SECOND INTERNATIONAL CONFERENCE ON INVENTIVE COMPUTING AND INFORMATICS, ICICI 2024, 2024, pp. 477–483, 2nd International Conference on Inventive Computing and Informatics (ICICI), S E A Coll Engn & Technol, Bangalore, INDIA, JUN 11-12, 2024.
[doi:10.1109/ICICI62254.2024.00083](https://doi.org/10.1109/ICICI62254.2024.00083).